

The Pennsylvania State University

The Graduate School

College of Engineering

Microwave Ignition of Green Monopropellants

A Thesis in

Aerospace Engineering

by

Brian P. Lani

© 2014 Brian P. Lani

Submitted in Partial Fulfillment

of the Requirements

for the Degree of

Master of Science

May 2014

The thesis of Brian P. Lani was reviewed and approved* by the following:

Michael M. Micci
Professor of Aerospace Engineering
Director of Graduate Studies
Thesis Advisor

Sven G. Bilén
Associate Professor of Engineering Design, Electrical Engineering, and
Aerospace Engineering

George A. Lesieutre
Professor of Aerospace Engineering
Head of the Department of Aerospace Engineering

*Signatures are on file in the Graduate School

Abstract

Research on a microwave ignition system was conducted at The Pennsylvania State University to investigate the possibility of replacing traditional catalyst beds with an alternative ignition scheme for green monopropellants. These highly energetic ionic liquids promise to offer higher performance, safety, energy density, and system simplification if an igniter could be developed to withstand the elevated combustion temperatures. The microwave igniter was built upon previous high-temperature microwave plasma torch research, using an optimized experimental setup to maximize the probability for monopropellant ignition under ambient atmospheric conditions. The ignition system propagates microwave energy at 2.45 GHz through rectangular waveguides in the TE_{10} mode where it encounters a tunable sliding short and establishes a standing wave. A conducting monopropellant feed line protrudes through the wide walls of the waveguide at an antinode location, amplifies the local electric field, and delivers the required breakdown energy into the propellant at 99% efficiency. Prior research indicates that the microwave energy deposited into the ionic liquid causes it to ignite due to a combination of ohmic heating and ion migration. The primary areas of interest during experimentation focused on: verification of ignition without a catalyst, demonstration of sustained combustion, optimization of propellant flow rate, and extension of torch lifetime expectancy.

The experimental setup for the microwave ignition system is described in detail. Initial tests progressed in steps toward monopropellant ignition by first demonstrating the formation of 3–4 inch plasma jets formed by pumping helium through the torch. Four separate formulations of monopropellant ignited and sustained combustion by injection into the helium plasma. The helium was then shut off and combustion of the monopropellants continued, proving that the torch could sustain ignition without the helium catalyst. The optimal flow rate for these tests was found to be between 2–6 mL/min of monopropellant at 500 W of input power.

Several issues were identified and addressed over the course of experimentation. Plasma exiting the torch at odd angles was found to be the result of imperfect tooling and was fixed with extra polishing methods. Burn duration was drastically increased by switching the propellant tubes from stainless steel to molybdenum. Electrical arcing from the torch tip to the aperture wall was eliminated by positioning the nozzle outside of the waveguide. Ignition of the monopropellant without preheating or injection into the plasma was hindered by unburnt propellant, or hot combustion gases, pooling in the waveguide when the ignition tests were performed vertically and upside down. Correction measures are currently being sought to prevent these fluids from entering the waveguide and robbing the torch of power. Recommendations for future experiments include increased diagnostics, examination of the air plasma, further experimentation without the preheat method, and tradeoff studies between optimal flow rate for combustion efficiency and lifetime expectancy.

Table Of Contents

List of Figures	vi
List of Tables	vii
Nomenclature	viii
Acknowledgments	ix
Chapter 1 Introduction	1
1.1 The Need for Environmentally Green Access to Space.....	1
1.2 Current Green Alternatives.....	4
1.2.1 <i>Safety</i>	4
1.2.2 <i>Storability</i>	5
1.2.3 <i>Performance</i>	6
1.3 Motivation for Microwave Ignition.....	6
1.4 Previous Research.....	7
1.5 Microwave Igniter Objectives	8
Chapter 2 Theory	9
2.1 Electromagnetic Transmission	9
2.1.1 <i>Electromagnetic Wave Propagation</i>	10
2.1.2 <i>TE Standing Waves in a Rectangular Waveguide</i>	13
2.2 Microwave Plasmas	14
2.2.1 <i>Plasma Criteria</i>	14
2.2.2 <i>Breakdown and Formation</i>	15
2.2.3 <i>Maintenance Processes</i>	16
2.3 Ionic Liquids	18
2.3.1 <i>Behavior of Liquids in a Strong Electric Field</i>	18
2.3.2 <i>Ionic Liquid Ignition Processes</i>	18
Chapter 3 Methods	20
3.1 Design Needs.....	20
3.2 Experimental Setup.....	21
3.2.1 <i>Microwave Generating System</i>	21
3.2.2 <i>Waveguide Assembly</i>	22

3.2.3	<i>Igniter Assembly</i>	23
3.2.4	<i>Propellant Feed System</i>	26
Chapter 4 Test Fire Procedure and Results		28
4.1	Validation of Helium Plasma Ignition.....	28
4.2	Ignition Validation with HAN- and ADN-based Monopropellants	29
4.3	Evaluation of Optimal Ignition Conditions	32
4.4	Test Fire Iterations	32
4.4.1	<i>Angled Plasma Column</i>	32
4.4.2	<i>Burn Duration</i>	33
4.4.3	<i>Nozzle Position</i>	34
4.4.4	<i>Ignition without Helium Plasma</i>	36
4.4.5	<i>Ignition without Preheat</i>	36
Chapter 5 Conclusion		38
5.1	Summary	38
5.2	Future Work Suggestions	39
References		41

List of Figures

Figure 1: Student handling 13% molar HAN and water	5
Figure 2: Rectangular waveguide geometry ²³	11
Figure 3: Terminated transmission line ²³	13
Figure 4: Power flow in a microwave discharge ²⁷	17
Figure 5: Waveguide assembly	22
Figure 6: Transmission system block diagram	23
Figure 7: Microwave igniter tip and side view	24
Figure 8: Injector schematic.....	25
Figure 9: Helium and IL feed system.....	26
Figure 10: Propellant feed system schematic.....	27
Figure 11: System block diagram	27
Figure 12: Helium plasma	29
Figure 13: Helium plasma and HAN sustained ignition.....	30
Figure 14: Helium plasma, Propellant 1 injection, and sustained ignition	30
Figure 15: Helium plasma and HAN-based Propellant 2 ignition.....	31
Figure 16: Helium plasma, ADN-propellant injection, and sustained combustion.....	31
Figure 17: Plasma column at exaggerated flow angle	33
Figure 18: Armature applying corrective pressure on the torch	33
Figure 19: Torch tip erosion.....	34
Figure 20: Electric field lines around a circular aperture with and without a central conducting post	35
Figure 21: Electrical arcing with nozzle at wall height.....	35
Figure 22: Ignition of ADN-based monopropellant after helium flow shut down.....	36
Figure 23: Electrical ignition of HAN-based monopropellant	37
Figure 24: Plasma and arcing occurring within the waveguide	37

List of Tables

Table 1: Standard rectangular waveguide data	12
--	----

Nomenclature

A_{mn}	Amplitude Constant
a	Wide Wall Waveguide Width, cm
β	Propagation Constant
b	Waveguide Height, cm
D	Total Diffusion Rate
E	Complex Electric Field Intensity, V/m
ε	Permittivity, F/m
f	Frequency, Hz
f_c	Cutoff Frequency, Hz
Γ	Reflection Coefficient
H	Complex Magnetic Field Intensity, A/m
k	Wavenumber, cm
Λ	Characteristic Diffusion Length, m
λ	Wavelength, m
λ_g	Guide Wavelength, cm
μ	Permeability, H/m
n	Electron concentration, m ⁻³
ω	Field Radian Frequency, rad/s
P_{av}	Average Power, W
P_{mn}	Power, W
t	Time, s
V_0^+	Incident Voltage, V
V_0^-	Reflected Voltage, V
v_i	Ion Production Rate
Z_L	Load Impedance, Ω
Z_0	Characteristic Impedance, Ω

Acknowledgments

I would like to take this time to recognize the many people who helped me throughout my graduate studies. First and foremost I would like to thank Dr. Michael M. Micci for sparking my interest in aerospace propulsion, providing me with research projects to practice those skills, and for encouraging me to continue my studies as a graduate student. His constant guidance and positive energy were the driving force behind this project. I would also like to thank Dr. Sven G. Bilén for his assistance and the expanse of knowledge he provided, especially during the challenging technical problems that arose. To Mr. Dillon for machining parts of the experimental apparatus.

Completion of this project also relied heavily on the strong support from all past, present, and future members on the plasma/propulsion team. Thank you to Mr. Timothy Stefanoski for his assistance and company in the lab. Thanks to Peter Hammond and Erica Capalungan for their guidance and previous research which led to this project.

Finally, I could not have undertaken this propulsion research without the love and support of my friends and family.

Chapter 1

Introduction

Since Robert Goddard's first flight of a liquid fueled rocket in 1926, military powers and space enthusiasts alike have strived to extend their reach towards the stars by developing improved propellants with increased performance.¹ Over the past century, improvements in liquid fuels have pushed performance by increasing the propellant specific impulse, density, and storability while optimizing the formulation for specific operational mission types and durations. Over the years, these fuels have evolved into highly energetic propellants, which are prized for their ease of ignition (with or without an oxidizer), high performance, reduced system weight, and mission flexibility.

Environmental concerns, however, have taken a back seat to improvements in fuel performance since the declaration of a space race in the 1950s. The corrosiveness and toxicity of propellants, their effects on the environment, and their damaging consequences to workers were considered a small bump in the road in the pursuit of space exploration. Today, society has a more vigilant watch on humanity's relationship with the environment and acknowledges the damaging impact caused by our historical technological progression. World leaders now recognize climate change, species extinction, ozone depletion, and carcinogenic toxins as major causes for concern. Major efforts have arisen within NASA and other foreign space agencies to reduce the effects that future space technologies will have on the environment: one such project is the development of green fuel technology to power the next generation spacecraft.

Currently, high energy density ionic liquids have been making breakthrough advances towards replacing the toxic propellants of choice, hydrazine and ammonium perchlorate (AP), with safer, environmentally friendly alternatives. Two such propellants, ammonium dinitramide (ADN) and hydroxylammonium nitrate (HAN), are monopropellant technologies that have been maturing and closing in on the technology readiness level of previous propellants. However, new ignition technologies need to be integrated into current thruster designs to handle the increased combustion temperature and progress the technology further. This thesis addresses a novel ignition approach that ignites HAN and ADN-based green propellants by the use of electromagnetic waves in a microwave torch.

1.1 The Need for Environmentally Green Access to Space

Hydrazine and AP, two of the most common propellants in use, are only the latest products to be utilized in a constantly evolving propellant market. The development and use of these hazardous fuels stemmed from the search for new propellants to fix the drawbacks of earlier systems.

The first liquid fuels, such as those used by Goddard, mixed petroleum derivatives such as gasoline and kerosene with liquid oxygen to achieve combustion. These fuels fall under the cryogenic class of propellants, which are still in wide use today in modern first- and second-stage engines such as the SpaceX Merlin engine. The petroleum derivatives, when pumped through the engine for regenerative cooling, partially burn and leave a problematic residue consisting of sulfur, olefins, and aromatics deposited in the fuel lines. Buildup in the turbo pumps and regenerative cooling feed lines leads to decreased performance and the possibility of engine failure.¹ The cryogenic class also contains the liquid oxygen (LOX)/liquid hydrogen (LH₂) propellant combination, which is actually the most environmentally friendly. However, liquid hydrogen is not sufficiently dense, which leads to a tank volume four times as large for a given propellant mass than for other fuel/oxidizer combinations.² In general, the cryogenic class as a whole suffers from leakage problems and boil off, which require the pressure of the system to be constantly monitored and the tanks incrementally refilled until launch. This eliminates the entire class from use on long-duration and interplanetary missions, with mission duration measured in years. Overall, the extremely low temperatures of the cryogenics make them hard to handle and eventually prompted the development of a class of storable fuels.³

Many of the first storable liquid propellants that were developed used nitric acid, a highly corrosive, toxic, oxidizing agent.⁴ Nitric acid was added to existing petroleum propellants, such as gasoline, to make it storable; however, the combination had combustion instability problems that would only be solved with the addition of aniline. The aniline had an additional benefit of being hypergolic with nitric acid, meaning that common jet fuel or gasoline with an aniline additive would ignite on contact with the nitric acid, eliminating the need for an igniter and improving restart percentages.¹

While various storable liquid fuels were being designed and tested in the early 1940s, the most prolific, storable solid rocket propellant, ammonium perchlorate, was beginning to replace potassium perchlorate as the oxidizer of choice. The discovery of AP led to the design of large solid propellant motors, which powered everything from the Polaris missiles to the Space Shuttle's solid rocket boosters.⁵ AP has been prized over the years for its great performance characteristics and is still commonly used today. However, its prolonged use through the decades has led to perchlorate contamination and considerable damage to the environment. In *Advances in Spacecraft Technologies*, Larsson and Wingborg describe a workshop organized in 2009 by the US Department of Defense that labeled AP as a key environmental, safety, and occupational health issue.⁶ The widespread use of AP has led to a dispersal of perchlorate anions into the environment where they find their way into drinking water supplies. The perchlorate becomes harmful to humans in high concentrations, where it is mistaken as iodine by the body and leads to thyroid gland issues. Apart from perchlorate leeching into the groundwater, AP combustion produces enormous amounts of hydrochloric acid, up to 580 tons of the concentrated corrosive agent for every launch of the Space Shuttle.⁶

Returning to liquid propellants, the late 1940s and early 1950s saw the extended use of a newly developed formulation, hydrazine, in various combinations as a versatile and storable mono or bipropellant.⁵ Hydrazine is characterized by extreme reactivity as a reducing agent and can thermally decompose in the presence of a common metal catalyst, allowing it to combust without an igniter. This provided ease of ignition, reliable performance, and the simplicity of requiring only a single propellant

tank onboard the spacecraft, which reduces system mass. Hydrazine's use as a monopropellant also allowed for thruster simplicity, repeatable firings, and reduced plumbing and parts. To increase the propellant's specific thrust, hydrazine could also be used in combination with an oxidizer such as nitrogen tetroxide in a bipropellant mode that would ignite the mixture upon contact within the combustion chamber. Anhydrous hydrazine's stability and storability has been favored in the space industry for a long time and has landed it prominent roles from the main fuel in the Proton rocket to the auxiliary power units on the Space Shuttle. Hydrazine fuel can be stored for long periods of time with little to no decomposition, meaning it finds a perfect role in satellite station keeping and long endurance missions. The propellant is insensitive to shock and friction and presents no explosive hazard compared to the first storable propellants.⁷

In the past few decades, however, hydrazine has been attracting more attention for its toxic properties than for its time-tested performance characteristics. To date, hydrazine is one of the most hazardous chemicals used in the space industry due to its toxicity, reactivity, and flammability. It has been listed by the American Conference of Governmental Industrial Hygienists and the International Agency for Research on cancer as a carcinogen.^{1,7} Direct contact can cause serious burns and lesions, so, during handling, the workers are required to wear full protective clothing including a self-contained breathing apparatus to avoid damaging the body's mucous membranes. In addition, the corrosive chemical can undergo a dangerous catalytic process when exposed to common metals such as iron, nickel, rust, and copper oxide. If an anhydrous hydrazine leak encounters a rusty bolt, sawdust, rags, paper, and other common materials it can burst into flame in the open atmosphere and burn like gasoline.⁷ However, the main problem that this propellant causes to spacecraft operations is its scrupulous handling procedures.

The seriousness of hydrazine's toxicity could be seen during the landing operations of the Space Shuttle. Upon landing, a 45–60 minute procedure to check for trace amounts of hydrazine and its oxidizer would begin. The procedure required about 150 trained personnel equipped in full protective attire and breathing apparatus to "safe" the orbiter by conducting toxic vapor readings around the fuselage and flush residual explosive/toxic fumes out of the payload bay and other cavities. After the area in and around the orbiter is safe, the crew can finally exit the vehicle.⁸

As these propellants evolved, the push for a more versatile, storable, and high performance fuel has led to increasingly toxic, corrosive, and carcinogenic fuels. The next generation propellant technology needs to address the environmental issues that the space race has neglected while continuing improvements in storability, specific impulse, and energy density. The creation of a low sensitivity, low toxicity, non-carcinogenic, and environmentally benign fuel that can perform similarly to current propellant technology would actually lower the cost of accessing space.⁹ This is because the cost of the propellant is small in comparison to the launch costs, but the cost of operations and handling of propellants is still a major concern when dealing with cryogenic and toxic propellants.¹ A less toxic propellant with simplified handling and transportation would reduce the cost for fueling operations. Therefore, the improved performance and increased safety of a next generation green propellant would lower mission costs and provide an environmentally friendly alternative to the current toxic technology. The European Space Agency recently studied the economic benefits of such a fuel and decided that it was worth investing in green hydrazine substitutes for future missions. Recent green fuel combinations on the horizon have

proven that the future trend in propellant technology seems to be a propellant that provides a benefit to launch costs and environmental stability.^{6,9}

1.2 Current Green Alternatives

In order for any green fuel to be considered as a viable alternative, it must be an environmentally benign propellant that performs comparably or better than the current hydrazine fuels that have come to dominate spacecraft mono- and bipropellant propulsion systems. The next generation green fuel must improve system simplification by minimizing risks associated with toxicity, thermal management, operational handling complexity, and hazardous contamination of the environment.⁶ Currently, the Air Force Research Laboratory (AFRL), NASA Glenn Research Center (NGRC), and the Swedish Space Corporation (SSC) are working on energetic formulations that could replace the traditional storable propellants with higher performance/lower toxicity compounds that meet those requirements for a next-generation green fuel. These efforts have focused on a new class of monopropellants consisting of fuel and an oxidizing salt dissolved in water to form a stable liquid monopropellant. The United States has focused on using an energetic formulation of hydroxylammonium nitrate (HAN) with a fuel such as alcohol, ethanol, or glycine in a water-based solution while Sweden's formula uses ammonium dinitranide (ADN) with methanol, ammonia, and water to create an ionic liquid monopropellant. Both fuels have made huge leaps in advancing their technology readiness level over the past years to prepare for demonstrator flights. Sweden's PRISMA mission successfully demonstrated ADN's improved performance over hydrazine during its debut launch and the United States hopes to follow with their HAN demonstrator mission slated to launch in 2015.⁹⁻¹³ The improvements in safety, storability, and performance of both of these new monopropellants are compared against hydrazine in the following sections.

1.2.1 Safety

A safe propellant is defined by its reduced risk to crew and handling personnel. This means a reduced risk of toxicity, explosive vapors, shock sensitivity, and hazardous environmental contamination. Ultimately, a safe propellant will reduce launch costs by simplifying handling and transportation procedures, reducing the cost of fueling operations, and limiting the amount of disposable waste.

Both propellants have significantly reduced toxicity when compared with hydrazine and are classified as relatively benign. The biggest advantage of the ionic liquid monopropellants in terms of safety is their formulation. The addition of water to these oxidizing salt/fuel mixtures attracts the energetic salt ions and acts as a binding agent, preventing them from escaping in a hazardous vapor.¹⁰ The non-carcinogenic, low toxic fuels reduce hazardous handling and cleanup costs. As seen in Figure 1, the only personal protection equipment needed to handle these propellants is simple protective clothing like safety goggles and gloves.

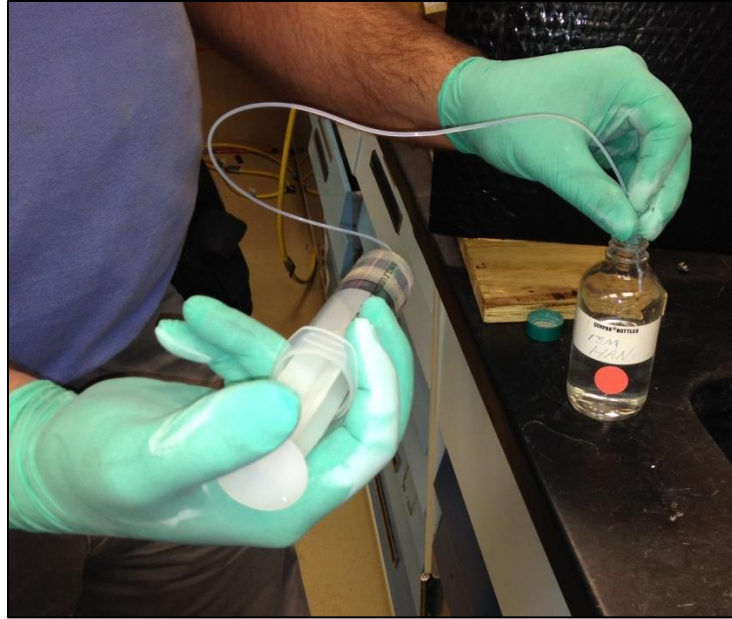


Figure 1: Student handling 13% molar HAN and water

In addition, their insensitivity to shock, friction, and sparking allows these green monopropellants to be transported on commercial vehicles including commercial air carriers to reduce shipping costs. On the PRISM project, all loading of the ADN-based fuel was declared non-hazardous operations by Range Safety and only required 3 kg of non-toxic waste removal compared to the 470 kg of toxic waste produced by the comparable hydrazine system. This meant the propellant, fueling, and transportation of the ADN-based propellant cost one-third as much as the same propulsion system using hydrazine.⁹⁻¹¹

1.2.2 Storability

Spacecraft need to hold fuel in their propellant tanks over the course of their mission lifetime. The mission duration, sometimes exceeding 10 years or more, is defined by the length of time during which they can use their fuel to station keep. When factoring in that many spacecraft are fueled weeks before launch, it becomes evident that the green propellants must be storage stable in a range of ambient temperature and humidity conditions over many years.¹³ Through extensive testing, both HAN and ADN have met the storability requirements and are not reactive with the common propellant tanks, meaning they can use predesigned tanks from previous propulsion systems. ADN has had the most extensive testing, with an ongoing test of a simplified version of a satellite propulsion system that has been running continuously for more than three years without any signs of degradation or pressure buildup. There are reports that indicate ADN-based propellants are storable for more than 20 years within the operating temperature.¹¹ The low freezing point of the monopropellants also allows the reduction of equipment by eliminating the need for tank and line heaters to keep the temperature of the fuel constant.

1.2.3 Performance

Over the past century, liquid fuels have drastically improved by increasing the specific impulse and propellant density, the key measures of rocket performance. Rockets and satellite propulsion systems are generally volume limited so it is crucial to optimize the fuel's volumetric energy. A high density propellant can extend the range of the propulsion system and reduce the need for large, heavy fuel tanks. The specific impulse, I_{sp} , is a measure of thrust provided for a given mass flow rate of the propellant. Because I_{sp} is proportional to the square root of the ratio of flame temperature to combustion-product molecular weight, the specific impulse parameter is maximized by a propellant with high combustion temperatures and low molecular weight.¹

When trying to determine the performance of ionic liquid propellants, the fuel component of the monopropellant, such as alcohol, ethanol, or glycine, determines the overall performance of the monopropellant. Therefore, fuel-heavy formulations within the ADN and HAN-based propellants will have the highest energy densities. HAN mixtures have been found to perform up to 25% better than hydrazine, but are currently limited to a smaller performance increases because of the existing catalyst technology.¹³ The HAN-based monopropellants have combustion temperatures well above hydrazine, which leads to a high specific impulse of up to 269 seconds.¹⁴ In addition, the HAN mixtures are 40% denser than hydrazine, which saves on tank volume.¹³ ADN mixtures have performed similarly, and with current thruster designs, achieved a 6% higher specific impulse and 24% greater density than hydrazine.¹¹ The increased specific impulse and density of these monopropellants means that the thrusters can have an extended mission and/or reduced tank volume.

1.3 Motivation for Microwave Ignition

Currently, monopropellants are passed over a catalyst bed to obtain ignition. However, the extreme combustion temperatures (≈ 2200 °C) of the higher-performance ionic liquid propellants pose significant problems to the current catalyst bed technology. Even state-of-the-art catalysts have not endured more than a few seconds of run time with the highest performing formulations of ADN and HAN.¹⁴ The common Shell-405 iridium catalyst has to be used with less energetic HAN and ADN formulations to reduce degradation of the catalyst bed and ensure thruster lifespan. The high combustion temperatures sinter the catalyst and rapidly decreases the catalytic surface area, leading to pressure spikes, and, if propellant flow is not stopped, an eventual pooling and subsequent detonation of the thruster.¹⁵

Current catalyst beds and supports would have to undergo extreme engineering changes for them to create a new system that can survive longer in this new combustion environment. However, even if these catalyst beds could be easily engineered, there would not be a single solution to all of the ignition problems. Aqueous ionic propellants are notoriously difficult to ignite (a safety feature) and require new ignitions schemes that have a higher ignition point. Research has also shown that different HAN, fuel, and water combinations require different ignition temperatures and reaction rates when passed over the same catalyst. For instance, a glycine-and-HAN combination that works well with one catalyst may work poorly when the fuel is changed to methanol. This implies that a separate catalyst needs to be

developed for each specific monopropellant formulation, increasing the cost because of specialization of parts for individual formulas.^{15,16}

Due to the difficulty of fabricating a single ignition system for each propellant formulation into a high-temperature catalyst bed, NASA has begun conducting studies on alternative ignition schemes such as laser-induced spark ignition and hot wire ignition.¹² Another ignition concept, which this thesis focuses on, is the ignition of HAN and ADN-based monopropellants with 2.45-GHz microwave energy, an industrial heating source. Microwave energy ignition systems do not rely on the chemical reaction between a certain catalyst metal and the monopropellant, thereby igniting all formulations of the aqueous solution indiscriminately. Since the performance of the ionic liquid monopropellants is based on the HAN/ADN-to-fuel ratio, the performance and energy density of the propellants could increase because very little of the microwave ignition system components come into contact with the high combustion temperatures. The PRISMA mission operated at half of its total specific impulse improvements over hydrazine because the catalyst bed was not developed enough for higher performance formulas.¹¹ A microwave ignition system would allow the thrusters to use the more energetic formulations of monopropellants to achieve maximum performance. Use of a microwave ignition system can also reduce overall thruster mass by elimination of the catalyst bed.

1.4 Previous Research

For over 20 years there has been active research into microwave ignition systems, generally used to ignite plasmas for industrial purposes such as material cutting, surface processing, and gas heating. These plasma torches operate by transferring microwave energy at 2.45 GHz, an industrial heating and the microwave oven frequency, to a propellant gas. Research on microwave torch efficiency since 2002 at The Pennsylvania State University has led to the development of an efficient torch referred to as the Penn State Microwave Plasma Torch (PSMPT). In this design, electromagnetic energy is transmitted through a waveguide to the jet of propellant emanating from the tip of a central conducting tube that protrudes from the walls. The intensified electric field at the tip accelerates electrons, which, in turn, transfer their energy to the gaseous propellant through collisions, creating an influx of charged particles and igniting a plasma.¹⁷ Microwave torches with this setup have been proven to sustain microwave plasma and microwave-to-plasma coupling efficiencies close to 100%.¹⁸ Further experimentation conducted in Penn State's Propulsion Engineering Research Center (now named the Center for Combustion, Power and Propulsion) has proven that HAN-based monopropellants can be ignited when irradiated by the microwave energy typical of these torches.¹⁹

It is assumed that the PSMPT can ignite ionic liquid monopropellants through two processes: ohmic heating and ion migration. Research on the Liquid Gun Program showed that the transmission of electrical energy through HAN-based monopropellant with a certain electrical resistivity produces heat. If the propellant absorbs enough heat it will rapidly decompose. The program continued its investigation into HAN-based propellant ignition and found that the electric field directs cations and anions dissolved in the solution into different directions. After the concentration of the nitrate ions reaches a tipping point, it initiates a chemical reaction that leads to ignition.²⁰ Both of these processes theoretically take place in the increased electric field at the microwave torch tip.

A recent study has found that the electric field generated by the microwave torch may also increase the completeness of combustion. In 2011, a group of researchers studying the benefits of applying electromagnetic energy to a combustion reaction discovered that it results in faster and more intense chemical energy conversion, increased flame stability, pollution reduction, increased fuel efficiency, and more reliable and rapid ignition.²¹ Their experiment used a microwave plasma torch to initiate and sustain the combustion of a premixed methane/air flame. They concluded that flame enhancement was caused by creation of radicals from collisions with electrons, radiation-induced electron excitation, increased flame temperature by ohmic heating, and production of excited species states—all of which point towards the microwave igniter as the perfect candidate for ionic liquid monopropellant ignition.²¹

1.5 Microwave Igniter Objectives

The objective of this research was to develop a microwave ignition system to bring about complete combustion of environmentally-friendly monopropellants and eliminate the use of catalyst beds in current thruster design. An economical design made use of proven technology from industry and commercial-off-the-shelf (COTS) parts to keep the cost of the ignition system on par with, or lower than, current catalyst systems. The microwave igniter was built upon the valuable lessons learned from previous research like the PSMPT and integrated new ideas for optimizing ignition conditions. Validation of successful ignition occurred in three steps: helium plasma ignition and stabilization, HAN and ADN-based propellant ignition by injection into the helium plasma, and monopropellant ignition without a helium plasma catalyst. Finally, the apparatus was used to evaluate the optimal ignition conditions and flow rates to sustain combustion. By progressing in this manner, the system could be tuned for maximum performance and minor issues could be identified and fixed before full-scale testing with the energetic propellants progresses.

Chapter 2

Theory

1.6 Electromagnetic Transmission

In order for electromagnetic energy to break down and ignite the monopropellant, it must first be transmitted from the power source, generally a magnetron, to the load torch. To understand this process, a basic understanding of transmission line theory and microwave engineering is required. Transmission theory defines the way electromagnetic signals propagate through space, conducting channels, or material media. It is connected with microwave engineering in that it explains which electromagnetic theories apply to the given transmitting system depending on the signal's wavelength.

When a signal's wavelength is long in comparison to the system's physical components, Kirchhoff's laws govern the electromagnetic transmission under the basic circuit theory. The basic circuit consisting of resistors, capacitors, inductors, and small lengths of wire form what is commonly known as a lumped-element circuit, in which components are much smaller than the electrical wavelength of the device. The wavelength can be calculated by dividing the speed of light in the medium by the wave frequency. Since circuit theory is generally considered valid up to a maximum frequency of 1 GHz, the corresponding smallest allowable wavelength would be 0.3 m. Because the wave is longer than the dimensions of any individual circuit component, there is negligible variation in phase across the element. Therefore, basic circuit theory states that each element observes a single phase and magnitude across both sides of the individual circuit component.

In the range of 1 to 100 GHz lies the microwave frequency band.²² The small wavelengths in this band set it apart from the others in the electromagnetic spectrum because the circuit components are the same length as the electrical wavelength. Thus the microwave transmission line can be modeled as a distributed set of microwave components with varying voltages and currents across circuit elements. In this arrangement, circuit theory does not apply and the general solutions to Maxwell's equations must be solved in order to find the solutions for electromagnetic propagation in microwave transmission lines.

Microwave transmission lines and waveguides must be constructed on length scales matching their respective wavelengths to allow electromagnetic propagation down the line. Consequently, simple metal tubes several centimeters in diameter were among the first waveguides invented to distribute microwave power from the source to the load. Over the past century several key forms of transmission lines such as waveguides, planar, and coaxial transmission lines were developed for specialized purposes. Each transmission line is characterized by its propagation constant and characteristic

impedance. If the line suffers a reduction of signal strength over long distances, then attenuation, or loss is also important characteristic.²³

Waveguides are a circular or rectangular metal tube that is capable of delivering low-loss transmission. Although they were the earliest type of microwave transmission line, they are still required in many applications that require high-power and precision. They also benefit from years of study, attenuation improvement, and commercial availability, which make them an affordable and reliable form of microwave transmission. Coaxial transmission lines shed the weight and rigidity of the waveguide and provide a cheap, broadband alternative. Planar transmission lines have increased in popularity as industry progresses with miniaturization and integration of microwave circuitry into active elements such as diodes and transistors. Planar transmission lines such as stripline, microstrip, slotline, and coplanar waveguides provide compact, inexpensive microwave communication.²³ With these options for possible transmission lines, the microwave igniter would benefit most from the high-power transmitting capabilities of the waveguide. The following sections will provide a more in depth discussion of the propagation properties of the rectangular waveguide.

1.6.1 Electromagnetic Wave Propagation

Waveguides are a type of transmission line that limits signal propagation to certain wave modes. Electromagnetic waves traveling through a transmission line may propagate as transverse electromagnetic (TEM), transverse electric (TE), and/or transverse magnetic (TM) waves depending on the type of transmission line and wave mode. Transmission lines composed of two or more conductors, such as the coaxial and planar lines, support TEM waves, which are defined as having neither electric nor magnetic fields in the direction of propagation. TEM waves have a clearly defined voltage, current, and characteristic impedance. Waveguides use a single conducting tube to propagate TE and/or TM waves. TE waves are characterized by a lack of electric field in the direction of propagation (H mode propagation), whereas TM waves lack a magnetic field in the direction of transmission (E mode propagation). Unlike the TEM waves, TE and TM waves cannot be defined by a characteristic impedance.

The waveguide's electromagnetic characteristics are largely dependent on the shape and dimensions of the tube. Figure 2 presents a schematic of a rectangular waveguide with dimensions $a \times b$, $a > b$, where z is considered the length of the transmission line. These dimensions will impact the propagation constant, cutoff frequency, impedance, and transmission power. For this analysis, the waveguide is assumed to have perfectly conducting walls to assist in equation simplification.

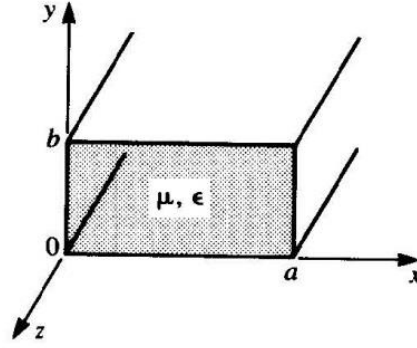


Figure 2: Rectangular waveguide geometry²³

To solve numerically for the waveguide's electromagnetic characteristics, Maxwell's equations must be simplified into a reduced wave equation for either the TE or TM mode by taking advantage of $H_z = 0$ and $E_z = 0$ in TE and TM waves, respectively. Using separation of variables, boundary conditions, and algebraic simplification, the propagation constant, β , can be determined by

$$\beta = \sqrt{k^2 - \left(\frac{m\pi}{a}\right)^2 - \left(\frac{n\pi}{b}\right)^2}, \quad (1)$$

where $m, n = 0, 1, 2, \dots$. The wavenumber, k , from Equation 1 is defined as

$$k = 2\pi f \sqrt{\mu\epsilon}, \quad (2)$$

where f is the source frequency, μ is the permeability of the medium, and ϵ is the permittivity of the medium. The propagation constant must be real in order for the waves to be transmitted through the waveguide. Examination of Equation 1 clearly shows that changing the frequency or dimensions of the waveguide would affect the propagation constant. If the frequency of a signal were to be incrementally increased in a waveguide with fixed dimensions, there would come a point at which the propagation constant becomes imaginary and microwave propagation ceases. The frequency at which this cutoff occurs is

$$f_{c_{mn}} = \frac{1}{2\pi\sqrt{\mu\epsilon}} \sqrt{\left(\frac{m\pi}{a}\right)^2 + \left(\frac{n\pi}{b}\right)^2}, \quad (3)$$

Transmission modes with cutoff frequencies lower than the operating frequency will propagate while those with cutoff frequencies higher than the operating frequency will exponentially decay as they travel. Equation 3 demonstrates that smaller waveguide dimensions support higher transmission frequencies.

Table 1 confirms this by presenting standard commercial waveguide dimensions and their corresponding cutoff frequencies.

Table 1: Standard rectangular waveguide data²³

Band	TE ₁₀ Cutoff Frequency (GHz)	EIA Designation WR-XX	Inside Dimensions (cm)
L	0.908	WR-650	6.500 × 3.250
R	1.372	WR-430	4.300 × 2.150
S	2.078	WR-284	2.840 × 1.340
H	3.152	WR-187	1.872 × 0.872

The equations listed so far are the same regardless of which TE_{mn} or TM_{mn} waves mode travel. However, it will become clear that there is an advantage to transmitting microwaves solely in the lowest cutoff frequency mode, i.e., the fundamental mode. Intuition says that setting $m=n=0$ in Maxwell's equations gives the trivial solution that requires all electromagnetic field components to equal zero, which means there is no wave amplitude. By examining the transverse field components of the TE mode, it is clear that lowest cutoff frequency is the TE₁₀ wave mode. Plugging in these values of $m=1$, $n=0$ into the cutoff frequency yields

$$f_{c_{10}} = \frac{1}{2a\sqrt{\mu\epsilon}}. \quad (4)$$

Applying this same procedure to the TM wave results in the values of $m=1$, $n=1$ because either $m,n=0$ would mean that its corresponding field expressions would all identically equal zero. This means the dominant TM₁₁ wave would have a cutoff frequency

$$f_{c_{11}} = \frac{1}{2a\sqrt{\mu\epsilon}} \sqrt{\left(\frac{\pi}{a}\right)^2 + \left(\frac{\pi}{b}\right)^2}. \quad (5)$$

By inspection, it is clear that the TE₁₀ wave has the lowest cutoff frequency and is, therefore, the overall dominant wave mode in the rectangular waveguide. This is important because it gives the waveguide a certain frequency range to dominantly transmit signals with the other modes in cutoff (or evanescence). Since the transmission velocity varies depending on mode, separate wave types traveling through the waveguide arrive at the output at different rates, which creates interference and distortion. In essence, transmitting microwave energy through a WR-284 rectangular waveguide with a single wave form, the TE₁₀ dominant mode, maximizes the power delivered to the microwave torch.

Equation 4 provides an additional interesting benefit of using the TE₁₀ wave. Since $n=0$ in the equation, the height of the waveguide, b , has no effect on the cutoff frequency. Yet higher modes of n will increase the cutoff frequency and exponentially decay. Decreasing the height also has the benefit of

increasing the local electric field strength on the transmission line for the TE₁₀ mode. For the TE₁₀ wave, the power transmitted through the waveguide in the dominant mode is²³

$$P_{10} = \frac{1}{2} \operatorname{Re} \int_{x=0}^a \int_{y=0}^b \overline{\mathbf{E}} \times \overline{\mathbf{H}} \cdot \hat{\mathbf{z}} \, dy \, dx = \frac{\omega \mu a^3 |A_{10}|^2 b}{4\pi^2} \operatorname{Re}(\beta), \quad (6)$$

where A_{10} is an arbitrary amplitude constant and ω is the field radian frequency. The propagation constant must be a real number in order for microwave transmission to occur. In practice, microwave energy is transmitted through a full-height waveguide until nearing the receiving device, where it then transitions to a half-height waveguide to increase the effective electric field at the component location. The microwave igniter transmits microwave energy through a series of standard WR-284 rectangular waveguides and transitions to half-height to intensify electric field strength only at the torch location to initiate plasma.

The half-height waveguide also has no impact on the wavelength, λ , of the transmitted signal. However the dimensions of the waveguide do have an impact on the guide wavelength, λ_g , which will always be longer than λ . They are defined as

$$\lambda_g = \frac{2\pi}{\beta} > \frac{2\pi}{k} = \lambda. \quad (7)$$

The electric field components of the TE₁₀ mode simplify so that it only has a magnitude in the y direction. The electric field varies within the waveguide as

$$E_y = \frac{-j\omega\mu a}{\pi} A_{10} \sin\left(\frac{\pi x}{a}\right) e^{-j\beta z}. \quad (8)$$

This equation can be solved for x to find the maximum electric field location along the waveguide width, a . This maximum electric field occurs at $x = a/2$, meaning that the torch nozzle should be placed in the center of the waveguide to have the highest potential for plasma breakdown.²³

1.6.2 TE Standing Waves in a Rectangular Waveguide

When microwave power travels from the generator to the circuit element, some of the incident power is absorbed while the rest is reflected. A model of a lossless transmission line terminating into a load of impedance, Z_L , is shown in Figure 3. In the microwave torch, the plasma forms the absorbing load.

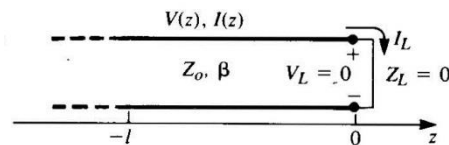


Figure 3: Terminated transmission line²³

Suppose an incident electromagnetic wave V_0^+ is generated by a source and sent along the transmission line. This wave has both a voltage and current, the ratio of which defines the characteristic impedance, Z_0 . Since the line terminates in an arbitrary load $Z_L \neq Z_0$ and the characteristic impedance should be equal to Z_L at the load. Thus an additional wave must be reflected from the load in order to satisfy this condition. Thus the voltage on the line could then be considered the sum of both the incident V_0^+ and reflected V_0^- waves.²³ Using this property, a voltage reflection coefficient Γ can be expressed as a ratio between incident and reflected voltages as

$$\Gamma = \frac{V_0^-}{V_0^+} = \frac{Z_L - Z_0}{Z_L + Z_0}. \quad (9)$$

There is no reflection of the incident wave when $\Gamma = 0$. The only way this can occur is if the load impedance is perfectly matched to the characteristic impedance of the transmission line. When $\Gamma \neq 0$, the superposition of the incident and reflected wave creates standing waves. The average power within the transmission line is given by

$$P_{av} = \frac{1}{2} \frac{|V_0^+|^2}{Z_0} (1 - |\Gamma|^2). \quad (10)$$

This equation demonstrates that the average power through the transmission line is constant. This result also shows that the delivered power to the device is equal to the incident minus the reflected power. 100% of the incident power is transferred to the load when $\Gamma = 0$ and no power is transferred to the load when $\Gamma = 1$. When the load is perfectly matched to the line, the voltage magnitude remains constant. However when there is a mismatched load on the line, the reflected wave generates standing waves, creating local maximum and minimums in voltage magnitude. The maximum voltage fluctuates with position along the line and forms local peaks separated by $l = \lambda / 2$. The voltage maxima locations can be calculated and an adjustable tuning short can fine-tune the length of the transmission line in order to move the voltage peaks to the desired location. The microwave torch is then placed within at the antinode to receive the peak power transfer from the conducting tube to the propellant.²³

1.7 Microwave Plasmas

A gaseous fluid in the presence of an increasing electric field will slowly become ionized until sparking, or breakdown, occurs. The plasma that forms is made up of charged particles that determine the conditions for sustained discharge and maintenance. The following sections focus on the microwave generated plasma's criteria, breakdown, and maintenance that will lead to propellant ignition.

1.7.1 Plasma Criteria

In an *Introduction to Plasma Physics and Controlled Fusion*, Chen defines plasma as a quasineutral gas of charged and neutral particles which exhibits collective behavior.²⁴ By this, he is referring to the plasma

as a collection of molecules that are not influenced by macroscopic forces. Instead, their motion is governed by electromagnetic forces acting on the plume, including the local fields that are generated by the movement of the charged particles within the plasma. As is shown in a later section, microwaves can travel through a plasma and produce electrons, maintaining the plasma formation. The charged particles also exhibit a Coulomb force that is magnified by the surrounding volume of charges. Because the elements of the plasma exert a force on each other over long distances, the motion of individual particles also heavily rely on the state of the plasma in the remote region. Therefore, the plasma exhibits collective behavior as each particle's movement is affected by entire group of charges.

According to Chen, an ionized gas must satisfy three criteria for it to be labeled plasma. The first specifies that the Debye length must be much greater than the dimensions of the plasma plume. Charged particles gathering around a local electric field within the plasma will shield distant particles beyond a certain distance, referred to as the Debye length. The shielding length must be less than the length of the plasma plume in order for distant charges to still have an effect on the individual particle, thus exhibiting collective behavior. The next criterion states that there must be enough charged particles within the plume to create this collective behavior. This requires a dense plasma cloud in order for the particles to "see" one another. The final criterion states that the charged particles should be free to oscillate many times before colliding with a neutral particle. Excessive collisions with neutral atoms would mean that the particle's motion is defined by ordinary hydrodynamic forces rather than electromagnetic forces.²⁴

1.7.2 Breakdown and Formation

In a gas with equal numbers of oppositely charged particles, the electrons are more rapidly accelerated by an electric field than the ions, making electrons the main species responsible for electrical breakdown. Any collection of gas contains a handful of free electrons that are the product of ionization by external sources. When a gaseous fluid encounters an electric field, the free electrons within the gas become energized. The electrons are accelerated in the direction of the electric field and inevitably collide with the walls or other molecules. During the collision, the electron is either lost to recombination with an ion or it imparts sufficient energy on an atom to release more charged particles. Increasing the electric field boosts the amount of secondary electrons generated by electron impact ionization until the gas becomes highly conductive. Any further increase in the electric field will suddenly cause the gas to glow and an electrical discharge, or spark, to shoot through the gas. The field magnitude required to produce this phenomenon is considered the breakdown field.

The Townsend criterion for breakdown numerically describes this tipping point. During a discharge, electrons are produced from electron impact ionization while others vanish by recombination, attachment, and diffusion. Matching the production rate to the loss rate creates steady state conditions. This is numerically shown in Equation 11 which expresses the electron concentration n as a function of the total diffusion rate D and the ion production rate ν_i . Therefore, the electron concentration can be defined as²⁵

$$n = n_0 e^{(v_i - D)t} . \quad (11)$$

Hence, an infinitesimally greater electron production rate throws the equation out of balance and leads to an exponential increase in electron density and gas discharge. Therefore, the Townsend criterion states breakdown occurs when electron production is matched by the loss rate.

A closer look at the electrical breakdown process shows that the collisions actually account for the energy balance as well as the charged particle balance. When exciting a gas with microwave energy, the frequency is so high that the electric field changes before the electron can travel any noticeable distance. This contains the electrons within the discharge area, while lower frequencies allow the electrons to freely leave. The fluctuating electric field accelerates the electrons into collisions with atoms, which, in general, change the direction of the electron but not its speed. However, the atom gains a fraction of the electron's energy through the collision before the changing electric field flings the electron in another direction. The electron continuously absorbs microwave energy and transfers it in small amounts to atoms through collisions, but its own total energy increases incrementally during microwave application. Some of these electrons will accumulate a kinetic energy greater than the lowest excitation energy of the atom. The energized electrons inelastically collide with the atom, splitting it into ion and electron. An electric field matching or exceeding the breakdown field will provide a runaway electron production rate leading to a current discharge. Consequently the microwave energy transmitted to the plasma torch does not need to be incrementally increased to get a discharge and plasma formation. Rather, turning on the microwave generator at the exact power required to match the electric breakdown field would produce instant ignition of the plasma.²⁵

The Townsend criterion can be mathematically expressed as a simple boundary value problem and used to find other interesting results. The pressure, microwave frequency, and ionization rates can be obtained by measuring the microwave breakdown in the gas and used to find the minimum electric field strength, or power, required to ignite the plasma. The efficiency of the energy transfer between the microwave input power and the electrons is also a function pressure. The torch is most efficient when the propellant pressure is high enough to result in many collisions of electrons with gas molecules per cycle.²⁶

1.7.3 Maintenance Processes

To maintain plasma there must be a power balance for electrons as well as a charged particle balance. Together, these ensure that power absorbed from the microwave energy balances itself with the power lost through collisions, resulting in equal creation and destruction of charged particles and a stable plasma.

The power balance per electron states that the power transferred to electrons from the electromagnetic field must equal energy lost per electron from collisions. The homogeneous Boltzmann equation can be viewed as a continuity equation in the electron energy space which equates the power transferred from the electric field per electron with random energy, u , to the power lost to electron–neutral and electron–electron collisions. The electromagnetic energy generated in the system is absorbed as kinetic

energy by the electrons, converted to internal molecular energy after collisions with molecules, and radiated from the plasma into the environment. The power flow from the generator to environment is shown below in Figure 4.

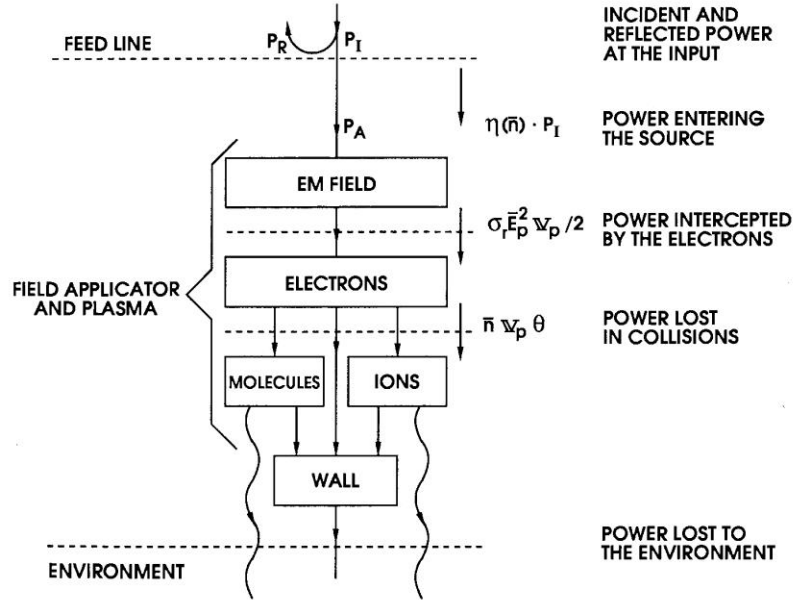


Figure 4: Power flow in a microwave discharge²⁷

When a steady discharge is established in a microwave circuit, it forms an absorbing load at the end of the transmission line. The plasma plume that forms at the end of the inner conductor provides more efficient power transfer from the waveguide to the plasma and ensures continued electron impact ionization. However, extra power delivered to the gas does not help to maintain the plasma. The power deposited into a plasma is directly proportional to the electron density. Therefore, any additional power absorbed by the plasma after the discharge is used to increase the electron density rather than increase the maintenance field amplitude.

The field amplitude established within the plasma is governed by the charged particle balance. As electrons collide with the wall, atoms, and other electrons, charged particles are created and others are destroyed or lost through diffusion, recombination, and attachment. The intensity of the electric field determines the collision frequency and, thus, the ion production rate. During the life of the plasma, the electric field amplitude in the plasma must adjust itself in order to guarantee that the ionization rate matches the average loss rate of charged particles to ensure it is a stable plasma. A simple formulation of the charged particle balance is

$$v_i = \frac{D_{se}}{\Lambda^2}, \quad (12)$$

where Λ is the characteristic diffusion length. The total diffusion coefficient reflects the free diffusion rate at low electron densities and ambipolar diffusion rate at higher ones.²⁷

1.8 Ionic Liquids

Ionic liquids are characterized by their low temperature melting point, electrical conductivity, and low viscosity. These characteristics make them a good fuel source in an aqueous monopropellant solution. Common ionic liquids used as monopropellants consist of a formulation of nitrate such as hydroxylammonium nitrate, ammonium dinitramide and hydrazinium nitroformate, and fuel such as alcohol, methanol, or glycine, mixed together with water in an aqueous solution. Electrical power dissipation into a monopropellant jet causes a temperature rise and spontaneous decomposition of the electrically conducting monopropellant.²⁸ Below we focus on the deposition of electromagnetic energy into HAN based monopropellants to bring about ignition processes.

1.8.1 Behavior of Liquids in a Strong Electric Field

A strong electric field will begin to breakdown a liquid and lead to an electric discharge only when the field energy density begins to match the external pressure. This is because the hydrostatic pressure arising in the liquid due to the intense electric field alters the liquid dielectrics. When an intense electric field is suddenly applied to the liquid, rarefaction waves reflect through the fluid and result in transient period where local density and pressure gradients form. The additional forces acting on the layers of the fluid result in a sharp pressure drop in the vicinity of the peak electric field at the nozzle tip. The resulting stress wave that forms heats the solution as it travels, boiling the liquid in certain regions and creating pre-breakdown bubbles. Because the boiling point is a function of pressure, the variations in pressure change the boiling point and the electric strength.²⁹ As an electric current is established in the liquid, ohmic, or resistive, heating becomes the prevalent source of the temperature rise. As the liquid boils, a vapor sheath forms at the nozzle walls which assists in arc formation.³⁰

1.8.2 Ionic Liquid Ignition Processes

The ignition sequence of ionic liquids like HAN-based monopropellants progresses through a unique set of phases when exposed to an electric field: pre-breakdown, expansion and contraction, thermal decomposition, and ignition and combustion. Because the electrical conductivity of the liquid is continuously changed by the internal pressure, many of these phases can be marked by the change in the electrical resistance of the propellant.²⁸

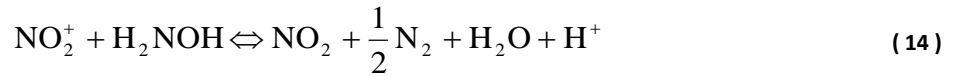
The pre-breakdown, or formative, phase describes the initial heating of the fluid in which the electrical resistance only slightly changes. As mentioned in Section 2.3.1, the ionic liquid passing through the intense electric field at the nozzle tip creates stress waves and resultant pressure gradients that generate a substantial amount of heat and boils the propellant. The resultant gas bubbles form a vapor sheath around the nozzle tip that assists in arc formation, causing an electric current to develop in the fluid. The passage of electric current through the conducting ionic fluid with a given electrical resistance releases thermal energy in a process known as ohmic heating.³⁰

After substantial heat is transferred to the monopropellant, the liquid undergoes a series of expansion and contraction processes. This phase, marked by a micro-explosion phenomenon, again occurs with little change in the electrical resistance of the monopropellant. The ionic liquid in the electric field oscillates at a random frequency and a small droplet will be splashed when the liquid phase temperature is about 126 °C. This is because of some small oscillatory decomposition of HAN creating gas cavities by superheating the low boiling point water in the mixture. The gas bubbles swell and burst randomly, creating a randomized expansion and contraction of the liquid.

Next, ion migration within the propellant leads to a sharp drop in resistance and signifies the beginning of the main thermal decomposition phase. The electric field separates the nitrate ions from the hydroxylammonium ions as they migrate in separate directions. Nitronium ions, NO_2^+ , are then formed as the local increased nitrate ion concentration shifts the chemical equilibrium of



to the right. It is the release of the nitronium ions that initiates the reaction sequences³⁰



which lead to combustion. The decomposition of HAN into reactive intermediates can be fully represented by Equations 13–15. Although nitronium ions start the ignition process, a self-sustained combustion process requires constant heating for the decomposition reaction to continue indefinitely. This additional heating is generally provided by the fuel component within the ionic mixture, such as alcohol. Interestingly, the fuel takes no part in the ignition process but determines the overall energy density of the monopropellant. The decomposition of HAN provides all of the intermediary particles needed sustain the chemical reactions.³⁰

Chapter 3

Methods

The proposed microwave ignition system was designed to ignite and sustain complete combustion of a fluid stream of HAN and ADN-based propellant without the use of a catalyst. The microwave igniter conceived for this role used 2.45-GHz microwave energy concentrated at a central conductor to ignite propellant. The microwave torch assembly consisted of three separate systems that worked together in order to provide IL ignition: the microwave generating system, waveguide assembly, and propellant feed system. An explanation of the design needs, experimental apparatus, setup, test fire procedures, and results are discussed further in this chapter.

1.9 Design Needs

The electromagnetic ignition system used in this experiment takes advantage of the lessons learned during previous research with high power plasma torches. The following objectives were identified as major design goals to provide the highest probability for monopropellant ignition and thruster integration:

- Generate an electromagnetic frequency that can excite plasma using proven technology and COTS parts;
- Provide required electromagnetic field distribution and intensity to initiate and sustain plasma;
- Ensure efficient power transfer from microwave generator to plasma;
- Deliver the correct flow rate to sustain ignition; and
- Support step-by-step monopropellant integration methods.

The microwave spectrum was chosen as the electromagnetic wavelength of choice because molecular, atomic, and nuclear resonances occur at microwave frequencies and efficiently heat the propellant by exciting molecules. Lower frequency induced plasmas like RF and DC tend to suffer from electron diffusion losses that hurt charged particle and, therefore, plasma production. As previously mentioned in Section 2.2.2, microwave frequencies efficiently trap electrons in the discharge zone, reducing the rate of ionization required to sustain plasma and transferring more energy to the propellant. Although higher frequency (≈ 30 GHz) microwave power provides exciting possibilities, previous research has shown that technical issues arise because the miniaturized parts they require have stringent machining tolerances, which negatively affects plasma formation when slightly skewed or worn down. The 2.45-GHz frequency was ultimately chosen because of its history of extensive research in producing gas

discharges and high density plasmas since the 1950s. As a benefit of this research, proven microwave technology has been in circulation for years. These inexpensive COTS microwave components and transmission lines allow for the creation of a robust microwave ignition system cheaper than current monopropellant catalyst technologies.²⁷

In order to provide the required electric field distribution and intensity to initiate plasma, the WR-284 rectangular waveguide was chosen as the transmission line to propagate the TE_{10} electromagnetic wave. As discussed in 2.1.1, the TE_{10} wave provides an electric field solely in the y -direction, parallel to the path of the central conducting tube that protrudes through the wide walls of the waveguide. A half-height waveguide at the location of this propellant tube intensifies the electric field. The TE_{10} wave continues to travel until it is reflected at the sliding short-circuit and creates a standing wave within the waveguide with an antinode at the torch location. Due to the energy accumulation in the standing wave, the resultant electric field at the torch tip is magnified and initiates breakdown.

To sustain the breakdown, the torch needed to continue efficiently transferring power to the plasma. Although the plasma itself forms an absorptive load, which increases efficiency, previous research has shown that the addition of an active three-stub tuner maximizes power transfer by matching the impedance of the fluctuating load.¹⁷ Also, a sudden increase in propellant flow rate would reduce the amount of ohmic heating provided to the fluid and drop the temperature away from its ignition point. Therefore, digital mass flow controllers regulated the monopropellant and helium over a wide range of flow rates to observe the optimum operating conditions.

Finally, the torch had to introduce and confirm the ignition of monopropellant in a step-by-step procedure. The goal of this was to observe helium plasma ignition and stabilization, HAN and ADN-based propellant ignition by injection into the helium plasma, and monopropellant ignition without a helium plasma catalyst. The torch used a Swagelok Tee to introduce either a single propellant, or both, to the torch depending on which ignition scheme was being explored. Each step put the experiment closer towards ignition without a catalyst and allowed for tuning and adjustment of the system as problems arose.

1.10 Experimental Setup

1.10.1 Microwave Generating System

Testing required microwave energy at a frequency of 2.45 GHz to be delivered to the microwave igniter through the waveguide assembly. To provide that power, the following equipment was utilized:

1. Daihen SGP-15A High-Voltage Power Supply Module;
2. Daihen SGM-15A Magnetron Module;
3. Daihen CMC-10A Controller Unit;
4. Daihen SMA-15A Automatic Microwave Tuning and Detector Unit;
5. Hewlett Packard E3615A DC Power Supply;
6. WR-284 Aluminum Waveguide; and
7. 3-Port Circulator.

The high-voltage power supply module provided DC power to the controller unit, automatic microwave tuning and detector unit, and magnetron module. By adjusting the dial on the high-voltage power supply, the unit could provide up to 1500 W of power to the magnetron. To disable the safety interlocks on the high-voltage power supply, the DC power supply had to apply 10 V to the unit before microwave output was allowed. Microwave energy generated by the magnetron at 2.45 GHz was first sent to the circulator. The passive three-port device transmitted signals only to the next port in rotation, thus allowing power sent from the magnetron to pass on to the tuner while reflected power from the system is dumped into a dummy load. This protected the magnetron from damaging reflected power. From the circulator the microwaves traveled to the automatic tuner and detector unit. The detector within the module measured forward and reflected power coming from the circuit. The tuner then matched the impedance of the circuit using a series of three prongs to maximize the power transmitted to the waveguide assembly. Microwave energy leaving the tuner entered a series of WR-284 waveguides to be transmitted the torch.

1.10.2 Waveguide Assembly

The waveguide assembly creates a circuit that concentrates and delivers microwave energy to the torch. The following equipment was used to transmit the energy to the microwave igniter:

1. WR-284 Aluminum Waveguides;
2. Half-height Reducing Waveguides;
3. Custom Modified Brass Waveguide;
4. WR-284 Sliding Short; and
5. Faraday Cage.

The microwave energy leaving the generating system enters a series of standard WR-284 waveguides. These COTS parts are widely available because they propagate energy at 2.45 GHz—a standard microwave oven frequency.¹⁹ From there the microwaves transition to half-height within the reducing waveguide. This reduction increases the electric field strength without changing the waveguide's transmitting wavelength or frequency. A modified brass waveguide holds the torch in this maximum electric field. The top contains a circular aperture where the torch tip projects out of the waveguide while the bottom has a brass holder to firmly hold the torch in place. The microwaves then transition back to full-height in another reducing waveguide before terminating at a variable sliding short. The short is a circuit-terminating wall that, when moved, shifts the standing wave within the waveguide. The short can then be used to tune the system by placing the standing wave maximum at the torch tip. The waveguide assembly is pictured in Figure 5. A custom-made Faraday cage rests on the modified brass waveguide to shield operators from microwave leakage through the torch aperture during test fires.



Figure 5: Waveguide assembly (source is connected to right side of structure)

The microwave generating system and waveguide assembly are attached to complete the microwave transmission system. The block diagram of this setup is featured in Figure 6.

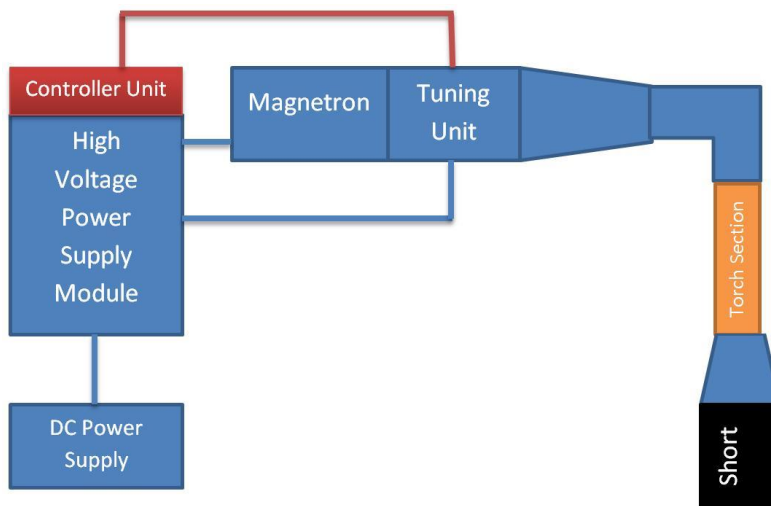


Figure 6: Transmission system block diagram

1.10.3 Igniter Assembly

The microwave torch was assembled from the following components:

1. Swagelok Tee;
2. Stainless Steel and/or Molybdenum Tubing; and
3. Conax Pressure Fitting.

As shown in Figure 7, the torch consisted of two stainless-steel hypodermic tubes with one positioned inside the other. The 0.042" OD, 0.035" ID inner tube carried the IL within the larger 0.12" OD, 0.10" ID tube that carried helium. Early on, drill bit blanks were used to center the inner stainless steel tube. Improved machining methods and an additional armature were utilized to ensure straight and centered tubes without the use of flow-blocking materials.



Figure 7: Microwave igniter tip and side view

A brass holder, silver soldered onto the bottom of the brass waveguide, secured the tubes and ran them up through the waveguide. The torch tip was positioned flush with the outer wall of the waveguide to obtain the peak electric field distribution. There, the stainless steel acts as a conducting post within the waveguide, which intensifies the electric field and provides electrical breakdown/ignition of the propellant. The propellant tubes ran out the bottom of the waveguide directly into a brass Swagelok tee that was hooked up to the propellant feed system. As modeled in Figure 8, the inner tube passes directly through the center of the Swagelok and exits the Conax connector. A plastic tube connected to the propellant feed system attaches to this thin metal tube and pumps IL directly through the torch. The larger stainless steel tube ends within the Swagelok tee. Helium entering the side port of the Swagelok flows through the outer hypodermic needle into the torch without interfering with the inner IL feed line.

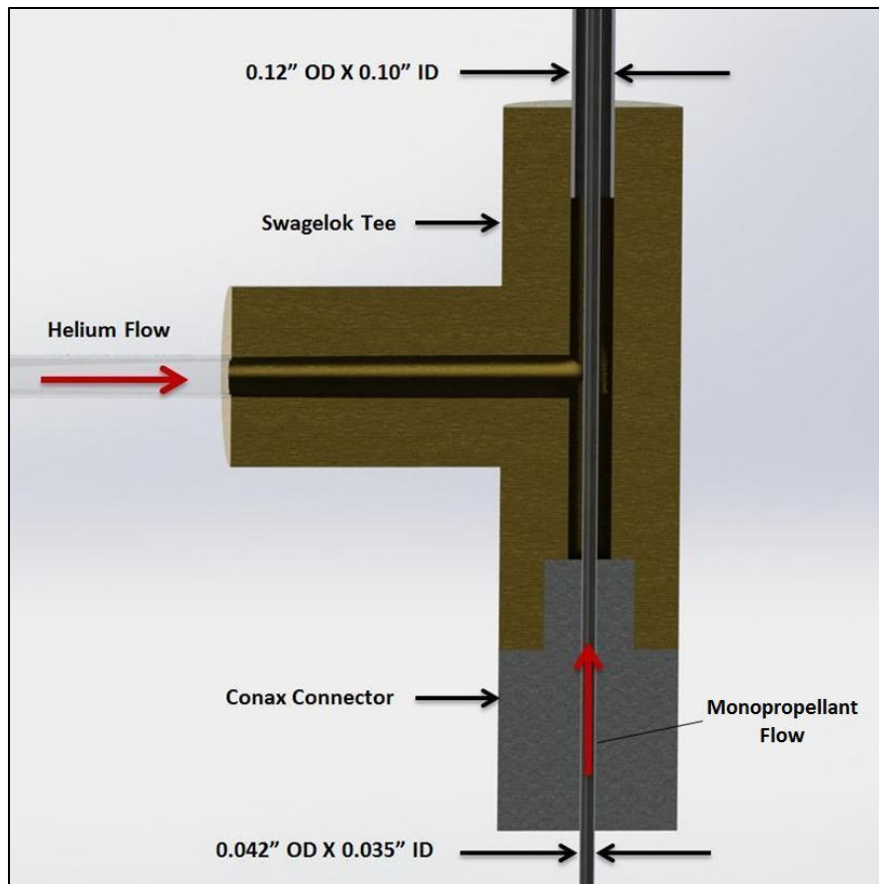


Figure 8: Injector schematic

Finally, the igniter assembly is held in place under the waveguide with the brass holder. Figure 9 shows the completed assembly with the torch inserted into the waveguide system. The torch tip is flush with the outer wall and the propellant feed system is attached to the IL and helium feed lines.



Figure 9: Helium and IL feed system

1.10.4 Propellant Feed System

A helium system and IL propellant feed system worked together to fuel the concentric tubing within the torch. This system used the following equipment:

1. Helium Compressed Gas Cylinder;
2. CGA 580 Regulator;
3. UNIT-Instruments UFC-8100 Mass Flow Controller (rated for 5 SLM nitrogen);
4. UNIT-Instruments URS-20 Control Box;
5. Plastic Tubing for Propellant Feed Line;
6. Syringe Pump; and
7. 60-mL Syringes.

The propellant feed system provided an outer flow of helium to create a plasma plume at the torch tip before IL pumping began. During operation, the syringe pump pushed IL through the inner needle while helium flow in the outer tube was controlled with the URS-20 control box. The IL feed system schematic is shown in Figure 10. The complete assembly is shown in Figure 11.

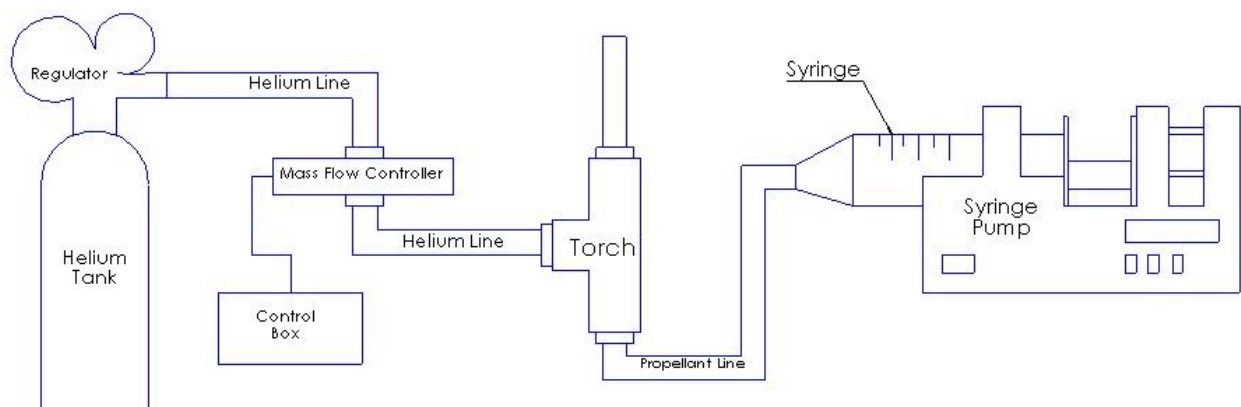


Figure 10: Propellant feed system schematic

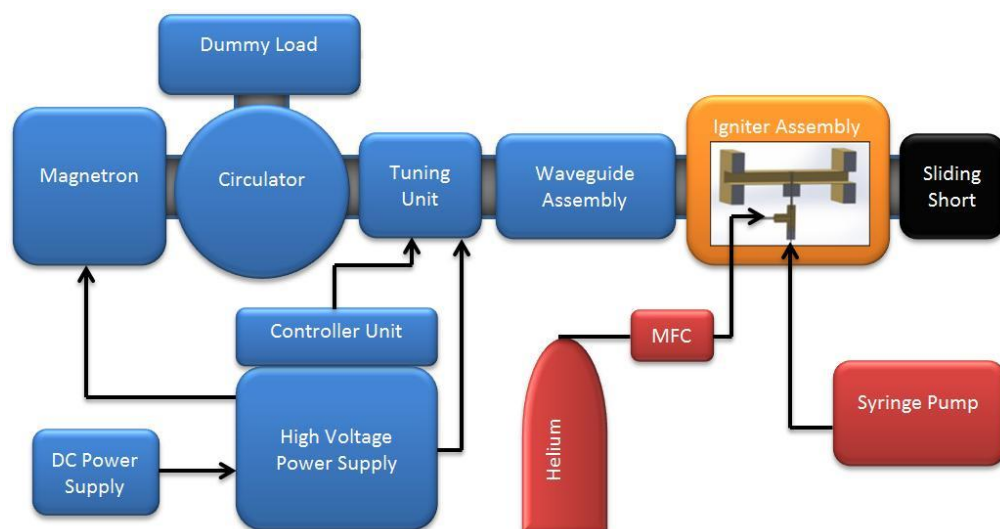


Figure 11: System block diagram

Chapter 4

Test Fire Procedure and Results

Testing sought to verify complete combustion of the IL under ambient atmospheric conditions. The first step in verifying the ignition system was to confirm that the setup could efficiently deliver the correct electric field amplitude to initiate and sustain a plasma discharge. To maximize the chance of ignition, the torch was initially test fired with helium to create a plasma jet at the tip of the torch before injecting the liquid monopropellant through the hot plasma. The torch would continue operation with both helium and IL propellants until multiple test fires proved that the monopropellant could be successfully ignited without the use of helium. Successful ignition with the torch using only the IL propellant would provide proof of concept for the microwave igniter. Continuous iterations on the initial experiment sought to identify optimal flow rates and modified configurations for maximum operational life of the microwave ignition system. This chapter provides a detailed account of test fire procedures and results.

1.11 Validation of Helium Plasma Ignition

Before the testing began, the tuning short was manually adjusted to position the internal standing wave, and, therefore, electric field maximum at the torch location within the waveguide. A custom Faraday cage was placed over the waveguide at the torch location to protect operators from microwave radiation leaking through the aperture. The DC power supply and high-voltage power supply module were turned on and the helium regulator valves opened. Using the URS-20 control box, helium was then flushed through the torch to remove air and increase the probability of plasma generation. After the two-minute purge, the helium flow rate was fixed at 12.08 mg/s and microwave power incrementally applied until a plasma jet formed at the torch tip. Early testing without a properly tuned short consistently led to plasma ignition at 500 W of incident power. This created a four-inch plasma jet exhausting vertically into the ambient air like the one pictured in Figure 12.

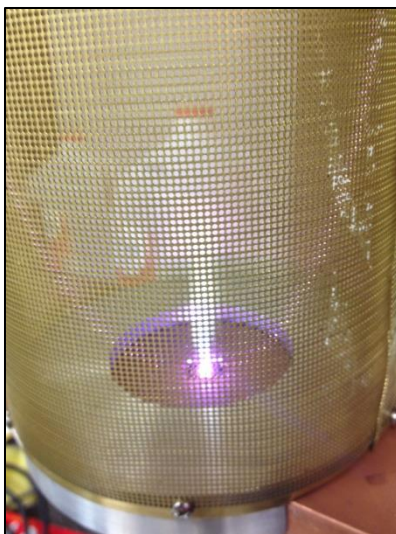


Figure 12: Helium plasma

As the microwave power was increased to the ignition point, the reflected power rapidly oscillated as the 3-stub tuner tried to match the impedance of the circuit. Upon breakdown, the plasma plume became an absorbing load for the circuit and provided efficient power transfer from the waveguide to the plasma. Reflected power dropped immediately upon ignition to about 1–3 W and proved that the system was routinely over 99% efficient at delivering the generated microwave power to the plasma. Later tests proved that a properly tuned torch could reduce the amount of microwave power required for plasma formation down to about 430 W.

1.12 Ignition Validation with HAN- and ADN-based Monopropellants

After initial plasma breakdown, the helium flow rate was increased to (70%) and allowed to stabilize into a steady helium plasma. This provided the base operating conditions with which to start the IL ignition sequence. Then the syringe pump was turned on and began metering IL through the torch. Ignition of the IL occurred instantaneously as it contacted the helium jet and was confirmed by visual cues such as increased flame length, color, and intensity. The IL propellant flow would continue for a short time before being cut off in order to verify that the intense flame was caused by the IL ignition. One ionic liquid formula tested in the torch was 13% molar HAN with water. The HAN flow rate, which was initially off during the test fire pictured in Figure 13, was increased instantaneously to 5 mL/min during torch operation. Ignition of the propellant can be noted by the brightness and color shift from the purplish-blue helium plasma to a bright reddish-yellow flame. After a period of around 30 seconds of sustained ignition, the HAN flow rate was cut and the flame returned to its initial purplish-blue helium plasma. The experiment was then repeated at a different IL mass flow rate to verify results and define optimal operational parameters.

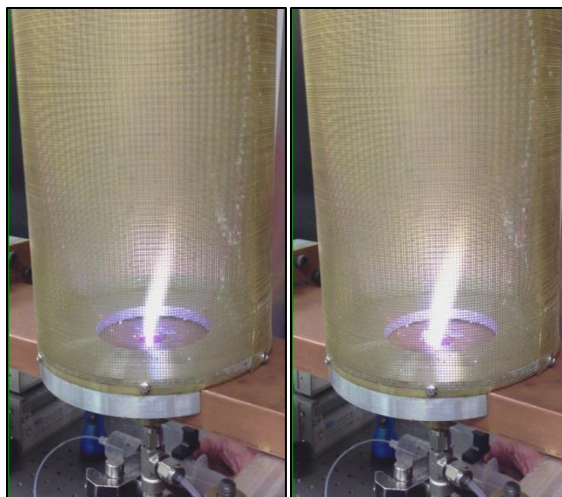


Figure 13: Helium plasma and HAN sustained ignition (from left to right)

Other ionic liquid formulations consisting of HAN and additional ingredients were tested to determine if similar monopropellants would have comparable, or possibly better, performance characteristics. Both propellant formulations with fuel additives provided more complete combustion and measurably larger flames than the 13% molar HAN with water mixture. One combination, referred herein as HAN-based Propellant 1, performed the best out of the HAN-based solutions. As pictured in Figure 14, Propellant 1 had the most noticeable increase in flame size and brightness throughout its ignition sequence and had the most complete combustion. The test fire pictured shows the progression through the three ignition steps from left to right: helium plasma ignition and stabilization, monopropellant ignition by injection into the plasma at 5 mL/min, and sustained combustion.

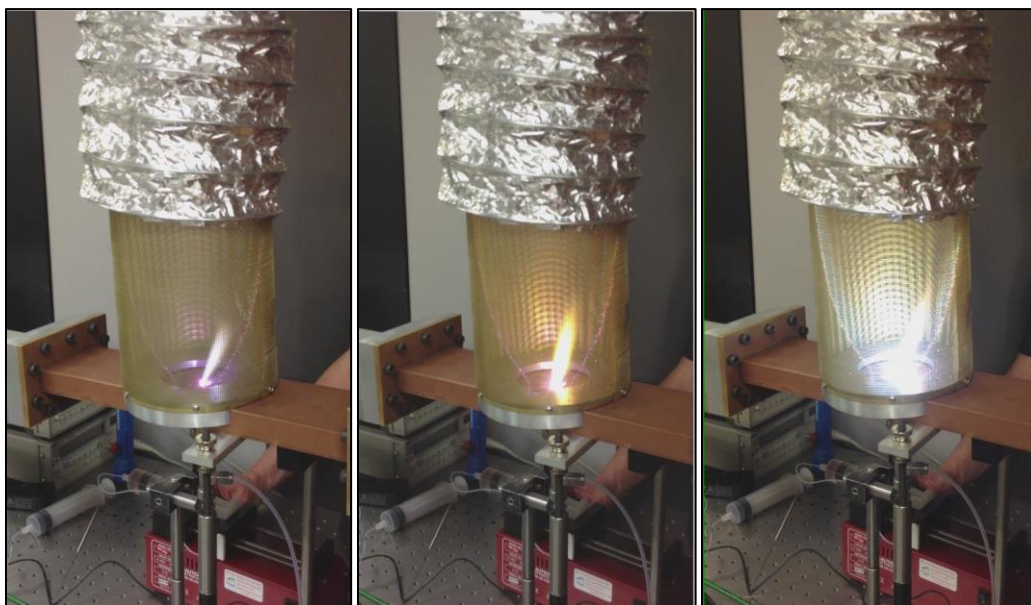


Figure 14: Helium plasma, Propellant 1 injection, and sustained ignition (from left to right)

The third and final HAN-based formulation, Propellant 2, performed similarly to Propellant 1. However, the high viscosity components within the ionic liquid seemed to have had a slightly negative effect on the size and brightness of the resultant flame when compared to Propellant 1. This could be due to the specific mixture of HAN, fuel, and water or it could be a result of decreased flow to the torch because the syringe pump sometimes faltered when forcibly pumping the viscous fluid through the small diameter tubing to the torch tip. The results of a test fire of this propellant at 5 mL/min are shown in Figure 15.

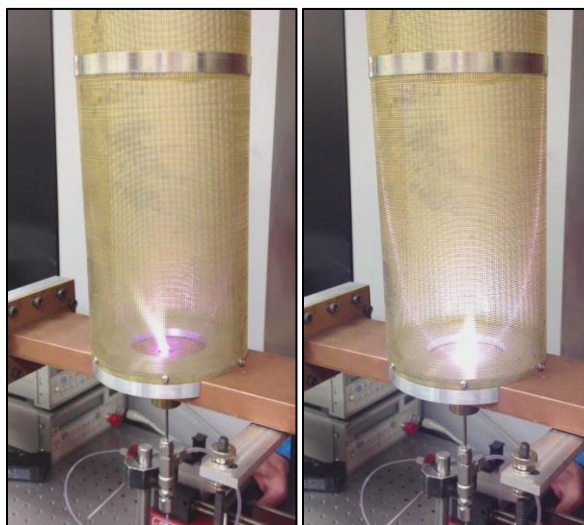


Figure 15: Helium plasma and HAN-based Propellant 2 ignition

In addition to the HAN-based fuels, an ADN-based monopropellant was test fired with the microwave ignition system. The ADN monopropellant behaved similarly to the previous formulations but slightly outperformed the HAN-based liquids in responsiveness and energetic reaction. However, residue on the top and of the cage and waveguide suggest that the fuel was not burned to completion. The test fire of ADN-based monopropellant is pictured below in Figure 16 as the propellant was pumped into the helium plasma at 2 mL/min.

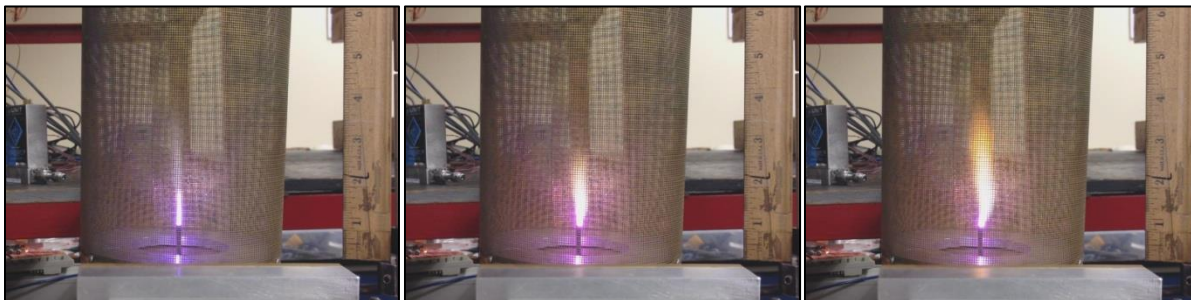


Figure 16: Helium plasma, ADN-propellant injection, and sustained combustion (left to right)

1.13 Evaluation of Optimal Ignition Conditions

With IL ignition confirmed over multiple tests, the flow rate was changed repeatedly to determine the optimal mass flow rate to sustain IL combustion. Tests performed with over 6 mL/min of IL tended to spew unburnt propellant all over the equipment. Excess propellant pooling within the waveguide absorbed microwave energy, heated up, and tended to flash ignite inside of the test apparatus. The unburnt propellant and residues in the waveguide would also absorb energy destined for the torch, decreasing the actual power delivered to the igniter. Eventually this reduced the torch's burning efficiency until the flame was extinguished and the input power went completely into heating the internal residues. Repeated testing narrowed the optimum flow rate for HAN based propellants to between 2–6 mL/min for sustained ignition with helium plasma at 500 W of input power.

The optimum flow of the ADN-based propellant was not explored due to an extremely limited supply. Optimal ignition conditions found for the HAN-based propellants were used for the ADN experiments, which had the highest likelihood of successful ignition without the helium plasma as seen in early ADN testing.

1.14 Test Fire Iterations

Over months of testing, iterations on the initial experimental procedure and equipment were performed to find the optimal operating conditions and smooth out some minor operational hiccups found during initial test fires. The goal was to further advance the microwave igniter concept to perform more reliably, for longer duration periods, and without additional helium propellant.

1.14.1 *Angled Plasma Column*

One unique problem that became evident during initial helium plasma formation was the tendency for the plasma column to exit the torch at an angle. Pictured in Figure 17, this phenomenon could potentially be problematic for a full scale thruster since the igniter would rest at the bottom of the combustion chamber. During operation the hot plasma could impinge on the cavity walls leading to uneven heat loading and wall erosion.

It was found that this phenomenon was caused by imperfect tooling of the stainless steel tubes and an off-center internal feed line. Tubes that were hand-cut with a Dremel tool initially had burrs and an uneven thickness around the torch tip. This partially blocked the flow and caused it to exit at an angle. The hot plasma melted through the thinnest section of the torch tip and exaggerated the flow angle. An off-center inner stainless steel tube would melt closed along the inside of the outer tube, which would further push the flow towards one side and prevent the IL propellant from entering the system. Hand reaming the tubes to remove burrs and create an even thickness around the torch tips partially solved this problem. An armature created out of mounting bars and brackets was assembled to apply pressure along the outside of the Swagelok tee and properly align the inner tube. This fixed the problem of proper torch alignment without using flow-blocking drill bit blanks which could also add to the problem. A picture of the armature is shown below in Figure 18.



Figure 17: Plasma column at exaggerated flow angle

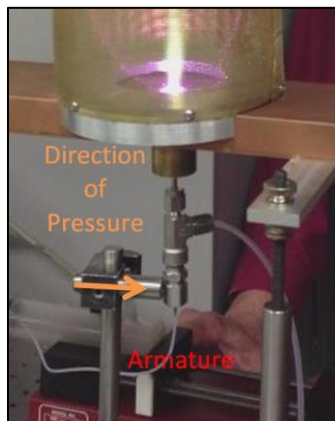


Figure 18: Armature applying corrective pressure on the torch

1.14.2 Burn Duration

Additional adjustments were made to increase the burn duration. Early tests were limited by the time it took to melt the stainless steel tubes down to within the waveguide. After reaching a certain level, the flame would be extinguished and the test could not be repeated until new tubes were machined and reset within the igniter. Torch tips, often badly mangled and enlarged by the test fires, had to be cut off so that the igniter could be removed from the waveguide assembly and reset. Nozzle erosion led to deterioration of the circular exit plane, distortions that altered the flow, shortened test duration, and inoperability of the monopropellant flow as the inner tube fused shut against the outer tube. An example of a used torch is pictured in Figure 19.

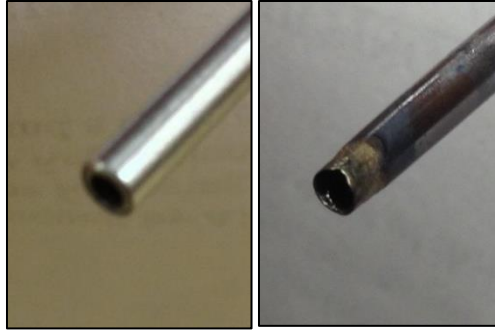


Figure 19: Torch tip erosion (before and after)

These problems were magnified when the system was properly tuned with the sliding short. Although ignition would occur at a lower power level, the stainless-steel tubes would burn down and extinguish the helium plasma before the IL propellant could be metered through the torch. This was the reason that the IL propellant was never test fired in the stainless-steel microwave igniter with a properly tuned system. The experiments highlighted a need for a stronger material to hold up against the brutal torch tip conditions. Thicker molybdenum tubing was chosen as a replacement for stainless steel because of its durability and high melting point (2620 °C compared to 1510 °C).³¹ By replacing the igniter tubes with molybdenum tubing, test fires could continue indefinitely. The new igniter was run for 10–15 minute durations without significant damage to the tip and was able to be restarted without machining and resetting new tubes within the igniter. Any melting of the torch tips happened at an even and almost unnoticed rate, even with the system properly tuned via the variable sliding short. All further testing continued with the system properly in tune.

However, one unexpected twist came with the removal of the stainless-steel outer tube from the system: the flame intensity seemed to decrease. Whether creating a helium plasma or burning monopropellant, the flame height was noticeably larger when using the stainless steel. It is believed that the melting stainless-steel tubes had been taking part in the reaction rather than simply guiding the propellants to their destination. As the vaporized stainless-steel merged with the IL and helium flow, it increased the amount of metallic ions within the fluid mixture. This changed the mixture's electrical conductivity and acted as a catalyst to enhance ignition properties and bring about complete combustion.

Nevertheless, molybdenum tubes repeatedly demonstrated their ability to successfully perform long duration test fires. The microwave torch could now repeatedly ignite helium plasmas at power levels as low as 430 W and could still sustain IL combustion using the normal startup procedures. The molybdenum reduced nozzle erosion and maintenance between test fires while increasing burn time and ignition reliability.

1.14.3 Nozzle Position

During some of the test fires, an intense electrical arc appeared to form at startup rather than a helium plasma column. The electrical arc connected the central conducting post (torch) to the side of the

circular aperture through which it protrudes. Figure 20 shows how the electric field lines around an aperture in a conducting wall should form. Normally, the electric field is magnified at the nozzle tip and breakdown creates an electrically conducting path away from the torch, resulting in a plasma. However, these field lines tended to arc from the nozzle tip to the waveguide aperture wall such as in Figure 21. The bright white spark would remain until enough of the torch tip had burned away to resume normal plasma formation. Previous tests had not sought a solution because the plasma would quickly form after the arc burned away the material. However, the switch to more durable molybdenum tubes meant the arc could burn away for an extended period of time before changing into the normal plasma column. The heat generated within the tube melted the inner IL propellant feed shut before testing could begin. Thus, a solution was needed at the torch tip to prevent the arc from forming.

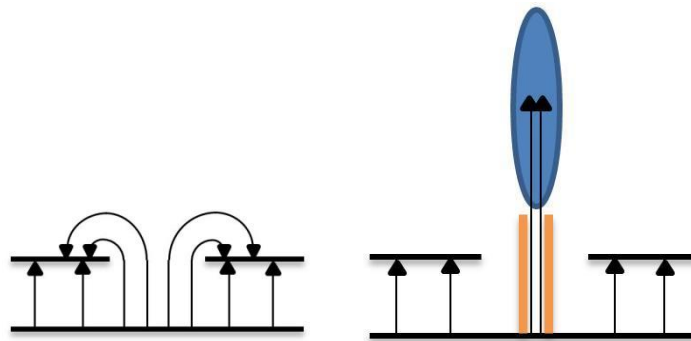


Figure 20: Electric field lines around a circular aperture with and without a central conducting post

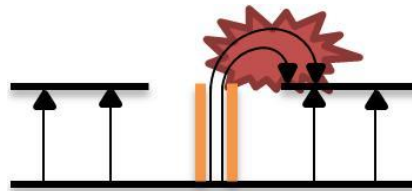


Figure 21: Electrical arcing with nozzle at wall height

Through all of the test fires described so far, the torch tip was placed approximately flush with the outer waveguide wall. The setup provided an easy and consistent waypoint for the torch tip location during repeated experiments. Previous research determined that the nozzle position could be optimized to maximize absorbed power, but concluded that the use of the efficient Daihen magnetron and automatic tuner system minimized the importance of nozzle tip location. This meant that the tip location could be moved vertically outside of the waveguide to provide separation distance from the circular aperture.¹⁷ With the nozzle located 3–4 cm above the waveguide, testing repeatedly produced plasma ignition under the standard startup procedures. To find the optimal nozzle location, the torch tip was then continuously moved from its maximum height to down halfway into the waveguide. The plasma stream was weaker when inside the waveguide and grew in intensity as it was moved up and out of the waveguide. When it was at flush with the outer wall (the initial test startup position), the arc occurred. Moving the nozzle vertically eliminated the arc and the normal plasma plume resumed. Repeated

testing with the igniter tip outside of the waveguide proved that the arc would no longer form and normal ignition would still occur.

1.14.4 Ignition without Helium Plasma

With the nozzle located outside of the waveguide, a test was run to determine if the new setup could sustain IL combustion without the use of helium. In early testing, helium flow was increased from 12.08 mg/s to (70%) to stabilize the plasma column before IL injection into the plasma plume. Previous research has shown that the increased mass flow rate decreases the plasma instabilities, resulting in increased combustion stability.¹⁷ Testing sought evidence of continued combustion of the IL monopropellant without the stabilizing helium plasma. To begin, the normal startup procedures were used to form a steady plasma column. IL propellant was metered in at 2 mL/min to confirm steady combustion before increasing the flow rate to 6 mL/min. From there, helium flow was shut off as the syringe pump continued feeding IL to the torch. As seen in Figure 22, the microwave igniter sustained combustion and continued operating even after the monopropellant feed line was unhooked from the igniter. The torch continued to burn the residual IL within the tubes until the microwave power was finally cut. This confirmed that the igniter could continue combustion of an energetic IL monopropellant without the use of stabilizing helium plasma after its initial ignition.

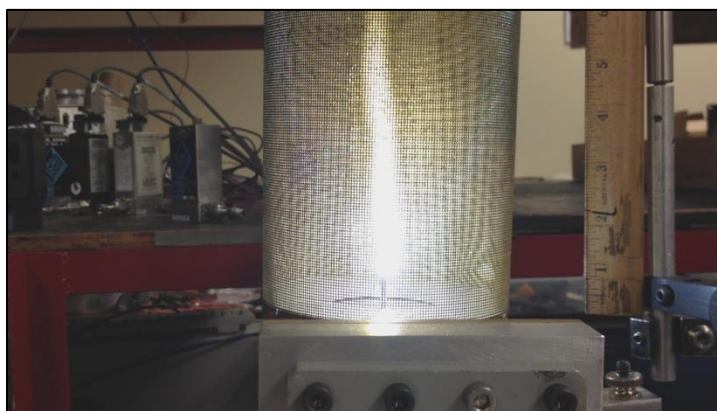


Figure 22: Ignition of ADN-based monopropellant after helium flow shut down

1.14.5 Ignition without Preheat

The final iteration sought to obtain startup ignition of a fluid stream of HAN-based propellant without the use of helium. The ignition and sustained combustion of an IL without a catalyst would provide proof of concept for the microwave igniter as a replacement for current catalyst beds. To maximize the chance of ignition, the test section was inverted to prevent the IL from pooling in the waveguide if the monopropellant did not instantaneously ignite. This allowed the setup to pump from the top and have the torch pointing downward to allow unburnt propellant to drip harmlessly into a collection bucket. With 500 W of incident power, IL propellant was injected into the torch at 2mL/min and flash ignited as seen in Figure 23. The flame would quickly extinguish and propellant continued to drip from the torch.

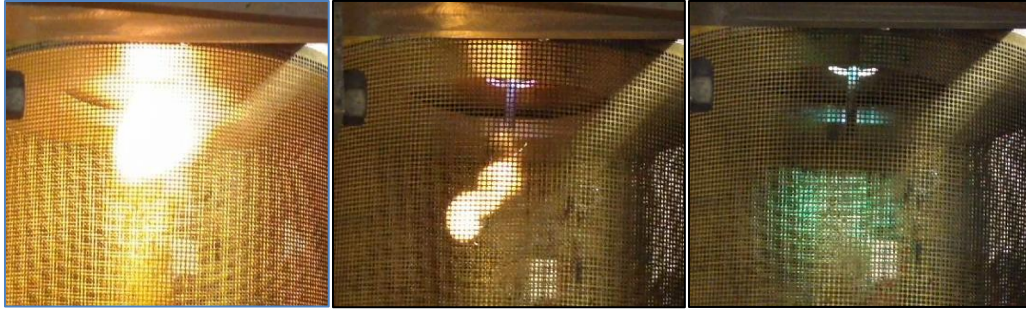


Figure 23: Electrical ignition of HAN-based monopropellant

Every so often the monopropellant would flash ignite again. Hot gases from the ignition rose and got trapped within the waveguide, robbing the system of power. When this happened, the power from the waveguide transferred to the pocket of trapped gases instead of focusing at the torch tip, reducing the probability of ignition at the torch location. While this plasma occurred within the waveguide (possibly with additional arcing at the nozzle-waveguide joint), the propellant continued to drip through the torch unburnt.

This phenomenon was seen in upside down test fires of helium plasma as well. Sometimes the normal steady plasma plume would form, while other times it would flash ignite and then the trapped pocket of helium in the waveguide would glow instead of keeping the torch lit. A picture of the faint glow during normal operation after the first flare up can be seen in Figure 24. It depicts a plasma or arc forming inside the waveguide at the opposite end of the conducting tube.



Figure 24: Plasma and arcing occurring within the waveguide

Chapter 5

Conclusion

1.15 Summary

The microwave igniter is a proof-of-concept device designed to initiate and sustain the combustion of high performance green monopropellants in ambient atmospheric conditions. A generator propagates 2.45-GHz microwave energy through a series of rectangular waveguides in the TE₁₀ mode in which they encounter a sliding short that creates a standing wave. Protruding through the wide walls of a half-height waveguide is a conductive nozzle that concentrates the local electric field to the point of breakdown. When a gas flows through the nozzle, free electrons are accelerated into collisions with other atoms in a cascade that creates a plasma plume 3–4 inches tall. Ionic liquids in the presence of the intense electric field jump in temperature through ohmic heating and ion migration, leading to combustion. The primary interest driving the microwave torch experiment is the need to engineer alternative ignition schemes to handle the extreme combustion temperatures posed by high-performance green propellants. A microwave ignition scheme could replace current catalyst technology with an igniter that could survive longer in the increased temperatures, ignite all IL formulations equally, and reduce system weight by elimination of the catalyst bed.

The experiment sought validation of plasma formation, confirmation of monopropellant ignition by injection into the plasma, and ignition and sustenance of combustion without the use of a catalyst through microwave ignition. The final goal was to determine optimal flow rates and lifetime expectancy of the experimental igniter. Initial testing proved that the microwave torch could efficiently provide the required electromagnetic field distribution and intensity to initiate and sustain a helium plasma. Operation of the torch with a properly tuned sliding short repeatedly generated four-inch plasma jets with as little as 430 W of incident power at 99% efficiency. Energetic ionic liquids were then injected into the plasma and ignited instantaneously as they contacted the helium jet. Ignition of four separate HAN- and ADN-based monopropellants were confirmed by visual cues such as increased flame length, color, and intensity. All formulations of the ionic liquids fared similarly under test conditions, yet HAN-based Propellant 1 and the ADN mixture stood out as the most energetic of the group, possibly due to their fuel additives. Helium flow was then cut while the monopropellants continued pumping through the torch. The large yellow flame that ensued survived until the system was shut down and confirmed that the monopropellant could sustain combustion without the helium catalyst. With ignition confirmed over multiple tests, the flow rate was repeatedly changed and the optimal flow rate was narrowed down to 2–6 mL/min for sustained combustion at 500 W of incident power.

While trying to advance the microwave igniter concept, the following problems were identified and corrected to permit the igniter to perform more reliably for longer duration periods:

- Plasma exiting the nozzle at an exaggerated angle was found to be the product of imperfect tooling. This was later fixed with additional machining and polishing steps in combination with an armature to precisely apply corrective pressure to align the torch.
- The burn duration was significantly increased by replacing the stainless-steel torch with tubes made of higher melting point molybdenum. This led to the discovery of the stainless-steel tubes' interaction and catalytic behavior with the monopropellant as the vaporized steel merged with the IL and enhanced the ignition properties.
- Another issue, electrical arcing between the torch tip and the aperture wall, was fixed by positioning the nozzle tip outside of the waveguide.

A final iteration sought to ignite the IL monopropellants without first preheating the torch tip with a helium plasma. The rig was turned upside down to allow excess fuel to drip away from the torch rather than collect within the waveguide and rob the torch of power. The test occurred at 500 W and observed 2 mL/min of monopropellant flash ignite before the hot gases rose, got trapped within the waveguide, and formed a plasma that directed all power away from the nozzle. Further testing is ongoing to try to find a solution to this problem.

1.16 Future Work Suggestions

Throughout the research conducted with the microwave ignition system, a number of experimental design improvements were noted that should be considered during future testing. Currently, there is an ongoing effort to examine the air plasma that forms when the helium flow is cut. This electrical discharge went unnoticed until a later test result showed that it produces a similar large yellow plume or flame that could be easily mistaken for the HAN and ADN combustion. Although this arc actually formed on the outside of the nozzle and rotated around the rim rather than forming at the tip of the nozzle, simple pictures and video of the test with a conventional camera do not pick up on this phenomenon and, therefore, cannot differentiate between a monopropellant flame and the air plasma. The electrical arc also accelerated the deterioration of the nozzle and used the microwave energy to ionize the air rather than ignite the propellant. A better understanding of the formation of the electrical discharge and its properties are needed to further our knowledge of the HAN/ADN ignition process and prevent other detrimental effects on the torch.

A more extensive quantification of the ignition process of the air discharge phenomena could be better examined with additional diagnostics. These are required to determine the exact burn composition, completeness of combustion, flame temperature, and percentage of burnt propellant. Spectroscopy would be useful in gauging flame temperature and allow for an overall estimate of total temperature in combustion chamber. Another test that captures and determines the exact composition of the combustion products could help verify the completeness of combustion and establish whether or not the microwave igniter is fully combusting the monopropellant or if most of it is being splashed out. Together, the flame temperature and product composition could be used to calculate the expected

thrust from a given rocket design at various mass flow rates. Spectroscopy could also be used to compare the heat of the plasma plume to that of the HAN or ADN monopropellant flame to verify ignition. Comparing the temperature of a regular HAN or ADN flame to that of a plasma assisted monopropellant flame could verify previous findings of enhanced flame properties and stand as proof of concept for the integration of a microwave igniter into a monopropellant thruster. Finally, a system should be developed to capture all of the residue and unburnt monopropellant that splashes out of the plasma stream. Comparing the collected unburnt monopropellant to the amount that was pumped through the torch would determine what percentage of propellant ignited. Performing this test over various flow rates should narrow down the optimum mass flow rate, or at least establish the efficiency of the igniter.

Further experimentation needs to be done on the ignition of the monopropellants without the use of preheating or injection into the plasma flame. Previous attempts were limited because firing in the vertical position pooled unburnt monopropellant in the waveguide and firing upside down trapped hot gases in the waveguide, both of which rob power from the torch and prevent it from igniting at the torch tip. A modified rig should be designed so that the combustion gases and unburnt propellant are directed harmlessly away from the transmission lines. This could mean test firing in a sideways position or under a slight vacuum. In these configurations, the monopropellants could be tested to determine if the flash ignition would turn into sustained combustion under different power levels and flow rates when product liquids/gases do not interfere with the experiment.

Finally, further research needs to define the optimal flow rate for IL ignition. This could be assisted by the increased diagnostics as previously mentioned, but a trade needs to be done to balance combustion efficiency with igniter life expectancy. For the microwave igniter to be adopted, it must be able to sustain ignition of the monopropellants longer than the current catalyst technology. Increased mass flow rates are desirable because they push the high temperature combustion products further away from the nozzle tip and increase total thrust, yet this thesis has shown that rates greater than 6 mL/min wastes fuel by sending unburnt propellant downstream. Therefore, a balance between life expectancy and total performance needs to take place in order to find the optimal flow rate for the microwave igniter.

References

- ¹ Edwards, Tim, "Liquid Fuels and Propellants for Aerospace Propulsion: 1903–2003," *Journal of Propulsion and Power*, vol. 19, no. 6, pp. 1089–1107, 2003.
- ² Hill, Philip G., and Carl Peterson. *Mechanics and Thermodynamics of Propulsion*, 2nd ed., Reading, Massachusetts: Addison-Wesley, 1992.
- ³ "Working of Cryogenic Propellants," *ThinkQuest*. Oracle Foundation [online database], URL: <https://gitso-outage.oracle.com/thinkquest> [accessed 21 January 2014].
- ⁴ "Nitric Acid/Kerosene," *Encyclopedia Astronautica* [online database], URL: <http://www.astronautix.com/props/nitrosene.htm> [accessed 21 January 2014].
- ⁵ Hunley, J. D. "The History of Solid-Propellant Rocketry: What We Do and Do Not Know," NASA H-2330, 1999.
- ⁶ Larsson, Anders, and Niklas Wingborg, *Green Propellants Based on Ammonium Dinitramide (ADN)*, *Advances in Spacecraft Technologies*, Dr Jason Hall (Ed.), ISBN: 978-953-307-551-8, InTech, 2011.
- ⁷ Simpson, D. K. "Safety and Handling of Hydrazine," Issue brief no. ADP005339.
- ⁸ "From Landing to Launch Orbiter Processing," NASA FS-2002-06-008-KSC [online database], URL: <http://www-pao.ksc.nasa.gov/kscpao/nasafact/pdf/orbiterprocessing2002.pdf> [accessed 22 January 2014].
- ⁹ Vasquez, Roger. "ECAPS Overview March 2013," *ECAPS 2013* [online database], URL: http://www.academia.edu/4143597/ECAPS_Overview_March_2013 [accessed 23 January 2014].
- ¹⁰ Hawkins, T.W., A.J. Brand, M. B. McKay, and M. Tinnirello, "Reduced Toxicity, High Performance Monopropellant at the U.S. Air Force Research Laboratory," U.S. Air Force Research Laboratory AFRL-RZ-ED-TP-2010-219, 2010.
- ¹¹ Neff, K., P. King, K. Anflo, and R. Moellerberg, "High Performance Green Propellant for Satellite Applications," *American Institute of Aeronautics and Astronautics*, 2009 [online journal].
- ¹² John, Blevins A., and Gregory W. Drake, "Developments of Ionic Liquid Monopropellants for In-Space Propulsion," Rep. no. 20050206333, 2005.
- ¹³ Reed, Brian, and Stephen Harasim, "Material Compatibility Testing with HAN-Based Monopropellants," *AIAA/ASME/SAE/ASEE 37th Joint Propulsion Conference and Exhibit*, 2001.
- ¹⁴ Reed, Brian D., "High-Performance Monopropellants and Catalysts Evaluated," NASA Tech. no. 20050192238, 2004.

- ¹⁵ Fortini, A.J., and J. R. Babcock, "High Temperature Catalyst Beds for Advanced Monopropellants," *AIAA/ASME/SAE/ASEE 37th Joint Propulsion Conference and Exhibit*, 2001.
- ¹⁶ Amrousse, Rachid, Keiichi Hori, Wafa Fetimi, and Kamal Farhat, "HAN and ADN as Liquid Monopropellants: Thermal and Catalytic Decomposition Processes," *Applied Catalysis B: Environmental*, vol. 137, pp. 121–128, 2012, doi: 10.1016/j.apcatb.2012.08.009.
- ¹⁷ Hammond, Peter J., "Investigation of a Microwave Plasma Torch," Ph.D. Dissertation, Aerospace Engineering Dept., The Pennsylvania State University, University Park, PA, 2013.
- ¹⁸ Youngtong-Gu, Suwon, "A Microwave Plasma Torch and Its Applications," *Plasma Sources Sci. Technol.*, vol. 15, pp. S26–34, 2006.
- ¹⁹ Davis, Chris, Michael M. Micci, and Sven G. Bilén, "PROPOSAL:F11B–T10–0251 Hybrid Chemical–Electric Propulsion (HCEP)," ElectroDynamic Applications, Inc., 2012.
- ²⁰ Klingenberg, G., H. J. Frieske, and H. Rockstroh, "Electrical Ignition of HAN-Based Liquid Propellants," Tech. no. ADA226314, 1990.
- ²¹ Hammack, Stephen, Xing Rao, Tonghun Lee, and Campbell Carter, "Direct-Coupled Plasma-Assisted Combustion Using a Microwave Waveguide Torch," *IEEE Transactions on Plasma Science*, vol. 39, no. 12, 2011.
- ²² Karmel, Paul R., Gabriel D. Colef, and Raymond L. Camisa, *Introduction to Electromagnetic and Microwave Engineering*, New York: Wiley, 1998.
- ²³ Pozar, David M., *Microwave Engineering*, Reading, Mass.: Addison-Wesley, 1990.
- ²⁴ Chen, Francis F., *Introduction to Plasma Physics and Controlled Fusion*, New York: Plenum, 1984.
- ²⁵ MacDonald, A. D., *Microwave Breakdown in Gases*, New York: Wiley, 1966.
- ²⁶ Herlin, Melvin, and Sanborn Brown, "Breakdown of a Gas at Microwave Frequencies," *Physical Review*, vol. 74, no. 3, pp. 291–296, 1948.
- ²⁷ Moisan, Michel, and Jacques Pelletier, *Microwave Excited Plasmas*, Amsterdam: Elsevier, 1992.
- ²⁸ Yu, Yonggang, Ming Li, Yanhuang Zhou, Xin Lu, and Yuzhu Pan, "Study on Electrical Ignition and Micro-explosion Properties of HAN-based Monopropellant Droplet," *Frontiers of Energy and Power Engineering in China*, vol. 4, no. 3, pp. 430–435, 2010.
- ²⁹ Ushakov, V. I. A., *Impulse Breakdown of Liquids*, Berlin: Springer, 2007.
- ³⁰ Klingenberg, G., H. J. Frieske, and H. Rockstroh, "Electrical Ignition of HAN-Based Liquid Propellants," Tech. no. ADA226314, 1990.

³¹ “Metals—Melting Temperatures,” *The Engineering Toolbox* [online database]. URL: http://www.engineeringtoolbox.com/melting-temperature-metals-d_860.html [accessed 29 January 2014].